Rap1 controls lymphocyte adhesion cascade and interstitial migration within lymph nodes in RAPL-dependent and -independent manners

*Yukihiko Ebisuno,[1] *Koko Katagiri,[1] Tomoya Katakai,[1] Yoshihiro Ueda,[1] Tomomi Nemoto,[2,3] Hiroyuki Inada,[4] Junichi Nabekura,[4] Takaharu Okada,[5] Reiji Kannagi,[6] Toshiyuki Tanaka,[7] Masayuki Miyasaka,[8] Nancy Hogg,[9] and Tatsuo Kinashi[1]

[1]Department of Molecular Genetics, Institute of Biomedical Science, Kansai Medical University, Monguchi, Japan; [2]Section of Multiphoton Neuroimaging, Supportive Center for Brain Research, National Institute for Physiological Sciences, Okazaki, Japan; [3]Laboratory of Molecular and Cellular Biophysics, Research Institute for Electric Science, Hokkaido University and JST, CREST, Sapporo, Japan; [4]Division of Homeostatic Development, Department of Developmental Physiology, National Institute for Physiological Sciences, Okazaki, Japan; [5]Research Unit for Immunodynamics, RIKEN Research Center for Allergy and Immunology, Yokohama, Japan; [6]Department of Molecular Pathology, Aichi Cancer Center, Nagoya, Japan; [7]Laboratory of Immunobiology, Department of Pharmacy, School of Pharmacy, Hyogo University of Health Sciences, Kobe, Japan; [8]Laboratory of Immunodynamics, Osaka University Graduate School of Medicine, Osaka, Japan; and [9]Leukocyte Adhesion Laboratory, Cancer Research UK London Research Institute, London, United Kingdom

The small GTPase Rap1 and its effector RAPL regulate lymphocyte adhesion and motility. However, their precise regulatory roles in the adhesion cascade preceding entry into lymph nodes and during interstitial migration are unclear. Here, we show that Rap1 is indispensably required for the chemokine-triggered initial arrest step of rolling lymphocytes through LFA-1, whereas RAPL is not involved in rapid arrest. RAPL and talin play a critical role in stabilizing lymphocyte arrest to the endothelium of blood vessels under flow or to the high endothelial venules of peripheral lymph nodes in vivo. Further, mutagenesis and peptide studies suggest that release of a trans-acting restraint from the β2 cytoplasmic region of LFA-1 is critical for Rap1-dependent initial arrest. Rap1 or RAPL deficiency severely impaired lymphocyte motility over lymph node stromal cells in vitro, and RAPL deficiency impaired high-velocity directional movement within lymph nodes. These findings reveal the several critical steps of Rap1, which are RAPL-dependent and -independent, in lymphocyte trafficking. (Blood. 2010;115:804-814)

Introduction

Lymphocyte trafficking plays important roles in immune surveillance and in adaptive immune responses. To better understand the regulatory mechanisms of these processes, it is important to determine how each trafficking step is controlled. Integrins are major adhesion molecules involved in dynamic lymphocyte trafficking. Central to these functions is the unique ability of integrins to regulate their adhesive activity by a process termed inside-out signaling. In addition, ligand-bound integrins transmit signals to the cytoplasm in an outside-in direction (outside-in signals), leading to stabilized adhesion, cell spreading, and modulated cellular functions.[1] It has been well established that temporal and spatial regulation of integrins through bidirectional signaling is important in adhesion-related cellular processes.[2,3]

Several well-characterized cellular processes critically involve integrins, including leukocyte trafficking to inflammatory sites and lymphocyte homing to secondary lymphoid organs. In the case of naive lymphocytes immigrating across high endothelial venules (HEVs) into peripheral lymph nodes (LNs), lymphocytes are first captured by weak binding between L-selectin and a sulfated sialyl Le^x-related carbohydrate, resulting in rolling on the HEV. When rolling lymphocytes are exposed to chemokines present on the luminal side of the HEV, chemokine signaling coupled with Gi proteins activates LFA-1 in less than 1 second, resulting in a complete stop (arrest).[4] Within seconds to minutes, lymphocyte adhesion is stabilized and these cells transmigrate into the tissues. The transition of integrin external domains from a bent to an extended conformation, which is triggered by separation of the α and β cytoplasmic domains,[5] has been proposed to transform rolling into arrest/adhesion.[6] However, our understanding of the molecular mechanisms of integrin regulation under physiologic conditions, where they occur over a broad range with a timescale of less than 1 second to minutes or hours, is still limited.

After transmigration, T cells enter the T cell–rich paracortex of the LN, which contains an elaborate network of fibroblastic reticular cells (FRCs), surrounding the HEVs and extending from the capsule to the medulla.[7] B cells migrate into the follicles where a dense network of follicular dendritic cells (FDCs) is organized. FRCs and FDCs produce homeostatic chemokines (CCL21, CXCL13, and CXCL12) and abundantly express integrin ligands, such as ICAM-1 and VCAM-1 as well as MAdCAM-1 in some areas.[7] Live imaging of the LN by 2-photon laser scanning microscopy has demonstrated a robust migration of lymphocytes in the paracortex and follicles.[8] FRCs and FDCs appear to support rapid movement of lymphocytes.[9] Although many studies reported that chemokines control integrin-dependent cell migration in vitro, it has not been determined whether integrins and chemokines coordinately regulate lymphocyte interstitial migration in lymphoid tissues. A recent study showed that immobilized chemokines

Submitted March 19, 2009; accepted October 31, 2009. Prepublished online as *Blood* First Edition paper, November 25, 2009; DOI 10.1182/blood-2009-03-211979.

*Y.E. and K.K. contributed equally to this study.

The online version of this article contains a data supplement.

The publication costs of this article were defrayed in part by page charge payment. Therefore, and solely to indicate this fact, this article is hereby marked "advertisement" in accordance with 18 USC section 1734.

sufficiently support T-cell migration without a major contribution by β2 and α4 integrins under shear-free conditions,[10] suggesting integrin-independent migration within the LN. DOCK2 is a Rac-GEF that is critical for actin cytoskeletal rearrangements in lymphocytes,[11] integrin activation and trafficking in B cells, and directional high-velocity lymphocyte movement in the LN.[12] However, the molecular mechanisms controlling interstitial migration of lymphocytes are largely unknown.

The small GTPase Rap1 is a potent activation signal for β1, β2, and β3 integrins and enhances cellular adhesion in both immune and nonimmune cells.[13] Lymphocyte Rap1, which is rapidly activated by chemokines and cognate antigens, increases the adhesiveness of integrins to their ligands by modulating affinity and avidity, induces polarized cell shape, and facilitates cell migration.[14] Targeted deletion of *Rap1a* and *Rap1b* resulted in impaired activation of lymphocyte and platelet integrins.[15-18] Although the phenotype of *Rap1a* and *Rap1b* double-knockout mice has not yet been reported, both Rap1a and Rap1b probably contribute to integrin activation. A deficiency in the Rap1-specific GEF, calcium, and diacylglycerol (CalDAG)–GEFI caused defective β1, β2, and β3 integrin activation in platelets and leukocytes in mice.[19-21] A splice junction mutation in this gene was reported in some LAD-III patients.[20] The signaling pathway of Rap1 activation by chemokines depends on PLC activity through CalDAG-GEFI to mediate human T-cell adhesion by LFA-1, but not VLA-4,[21] suggesting that multiple pathways regulate integrins. RAPL is highly expressed in immune cells where it functions as a Rap1-GTP–binding protein that mediates Rap1 functions on integrins.[22] Targeted deletion of the *rapl* gene impaired chemokine-induced lymphocyte adhesion and trafficking to peripheral LNs.[23] However, the exact roles of Rap1 and RAPL signaling in lymphocyte adhesion cascades on endothelial cells and interstitial migration after entering the LNs are unknown. Here we demonstrate the essential steps of Rap1 and RAPL signaling in lymphocyte trafficking.

Methods

Methods for mice, plasmids, cell transfection, shRNA knockdown, flow and motility assays, intravital microscopy, and flow cytometric analysis are provided in detail in supplemental Methods (available on the *Blood* website; see the Supplemental Materials link at the top of the online article). Mice were housed in specific pathogen-free conditions, and all experiments were conducted in accordance with protocols approved by the Animal Care and Use Committee of Kansai Medical University (Osaka, Japan).

Results

Establishment of an in vitro system to reproduce the lymphocyte adhesion cascade

Most of the previous studies examining LFA-1 activation processes were performed by first reproducing the transition of selectin-dependent rolling into chemokine-triggered arrest by integrins. Therefore, our approach was to reconstitute the lymphocyte adhesion cascade mediated by L-selectin and LFA-1 using a BAF pro-B-cell line expressing human L-selectin and LFA-1 (BAF/LFA-1/L-selectin) and LS12 endothelial cells expressing tumor necrosis factor-α (TNF-α)–induced ICAM-1, as well as the L-selectin ligand, PNAd, which was produced by introducing HEV-specific carbohydrate modification enzymes.[24] When infused over the monolayer of LS12 cells immobilized with CXCL12 in the parallel plate flow chamber at various shear stresses, a fraction of BAF/LFA-1/L-selectin cells exhibited rolling at various velocities and stopped at the shear stress between 1 to 5 dyne/cm^2. We found that shear stress less than 0.6 dyne/cm^2 did not support lymphocyte rolling, consistent with a previous report demonstrated for primary T cells.[25]

Because the transition from rolling to arrest was efficiently observed when cells were infused at 2 dyne/cm^2 into this system, the experiments hereafter were performed at this shear stress. The images of cellular interactions were acquired by a CCD camera and video-recorded, and then digitized at 30 frames/second and subjected to an auto-cell tracking analysis. The representative adhesive profiles are shown (Figure 1). The attachment sustained for more than 10 seconds (typically longer than 1 minute) is hereafter termed "stable arrest" (Figure 1B-C; supplemental Video 1). Treatment with pertussis toxin severely inhibited "transient arrest," attachment of less than 10 seconds, suggesting that it is a Gi-dependent process (data not shown). In the absence of chemokines, the majority of cells just rolled (Figure 3B; supplemental Video 10). Anti–L-selectin antibody (MEL-14) treatment abolished all cellular adhesion events (Figure 1B,D; supplemental Video 2). Treatment with anti–LFA-1 monoclonal antibody (TS1/22) abrogated arrest without affecting rolling (Figure 1B-D; supplemental Video 3). A similar result was also obtained with anti–ICAM-1 mAb (data not shown). Collectively, these results confirm that the in vitro flow system using BAF/LFA-1/L-selectin and LS12 cells recapitulates the lymphocyte adhesion cascade on HEV in peripheral LN in which endothelial chemokines convert L-selectin–mediated rolling into arrest by activating LFA-1.

Requirement for Rap1, RAPL, and talin in arrest by LFA-1 and ICAM-1

To clarify the roles of Rap1, RAPL, and talin in the arrest step, we knocked them down by more than 95% using lentiviral transduction of shRNAs specific for Rap1a, Rap1b, RAPL, and talin (Figure 1A). We also knocked down both RAPL and talin (Figure 1A right). The depletion of Rap1 in BAF/LFA-1/L-selectin completely inhibited chemokine-induced arrest without affecting rolling (Figure 1B-C; supplemental Video 4). The range of rolling velocities of Rap1 knockdown cells was almost identical to that of control cells treated with the anti–LFA-1 mAb (Figure 1D; supplemental Videos 3-4), indicating that Rap1 is critically involved in the transition from rolling to arrest. On the other hand, the knockdown of RAPL or talin did not significantly affect the transition to arrest, as the majority of cells stopped on the monolayer. However, the attached cells were easily dislodged, resulting in an increased transient arrest population with a reciprocal decreased stable arrest population (Figure 1B-C; supplemental Figure 1). The stopping time of cells depleted of RAPL or talin was less than 10 seconds with an average of 2.6 and 3.1 seconds, respectively (Figure 1B,C,E; supplemental Video 5). Double knockdown of RAPL and talin synergistically decreased the conversion to stable arrest and stopping times, suggesting that they have distinct effects on the arrest (Figure 1B,E). These results suggest that LFA-1–dependent arrest can be divided into 2 sequential steps. The initial step is a transition from rolling to arrest, occurring within 1 second, and requires Rap1. The subsequent stabilization occurs within 10 seconds and requires both RAPL and talin.

Previous studies suggest that conformational changes alter the affinity of LFA-1 and are required for LFA-1–dependent arrest. The conversion from the low affinity bent conformation to the intermediate affinity extended conformation induces the transition from rolling to arrest.[6,26] We examined whether the extension status of

LFA-1 could be regulated by Rap1, RAPL, and talin using the antibody KIM127, which recognizes an extension reporter epitope on the β2 subunit. The expression levels of the extension reporter epitope were significantly up-regulated by CXCL12, as previously reported,[27] indicating that this chemokine induces or shifts equilibrium to the extended conformation (Figure 1F; supplemental Figure 2). Neither Rap1 nor RAPL depletion affected KIM127 epitope expression. Depletion of

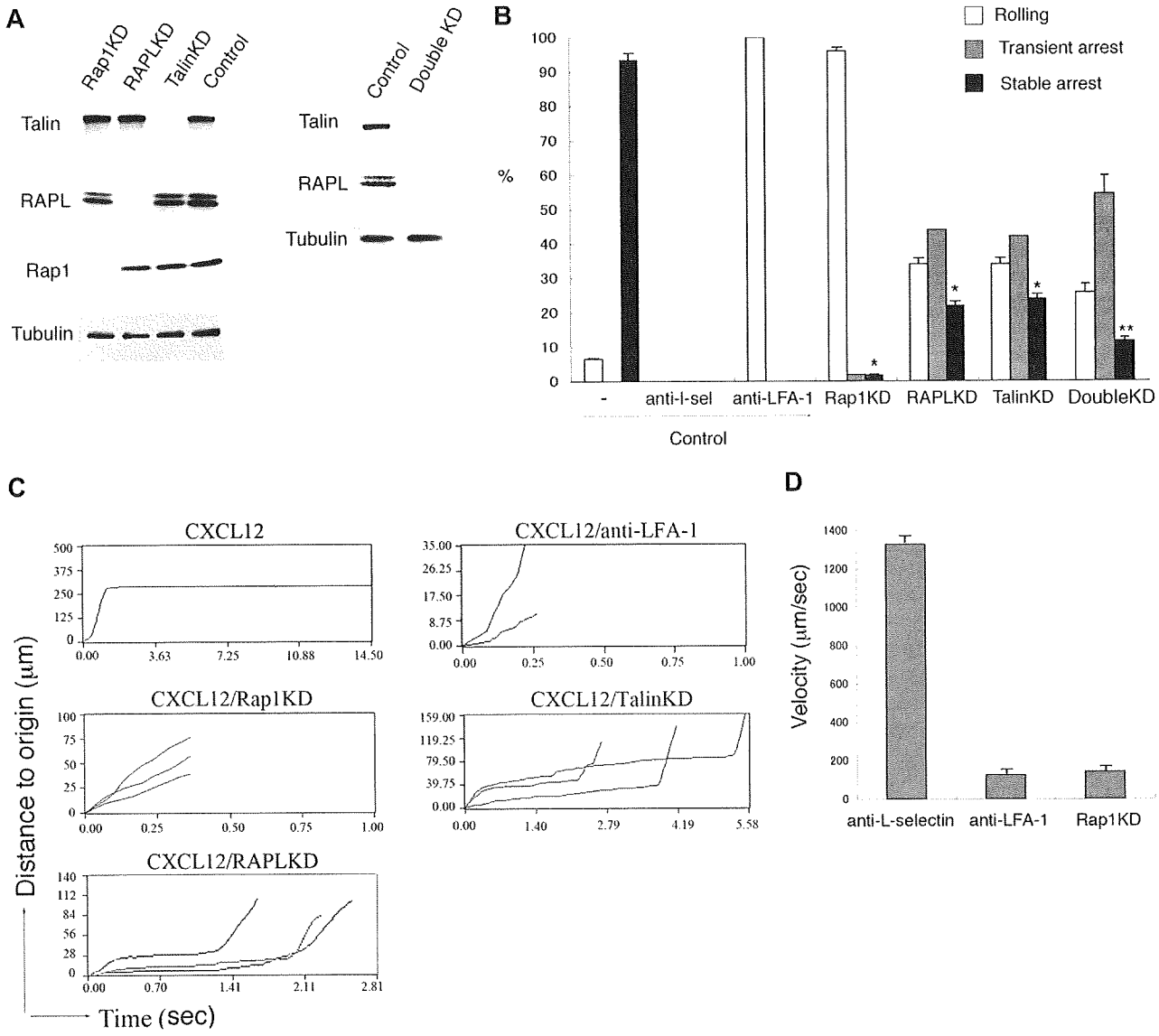

Figure 1.

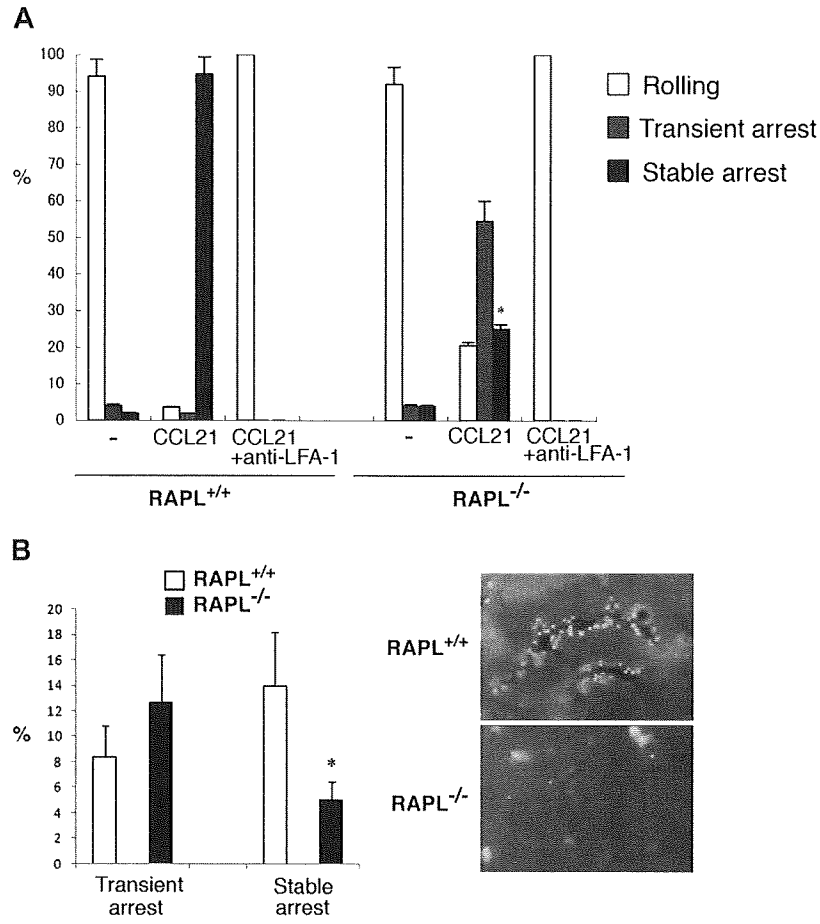

Figure 2. RAPL is required for stable adhesion. (A) The adhesion of wild-type and RAPL-deficient T lymphocytes with LS12 cells expressing mouse ICAM-1 under shear flow. Adhesive interactions were measured as in Figure 1. Data represent the mean ± SD of 3 independent experiments. $^*P < .001$, compared with wild-type lymphocytes. (B) Intravital microscopic analysis of wild-type and RAPL-deficient lymphocytes in HEVs. The percentages of transient arrest and stable arrest of adoptively transferred lymphocytes from control and RAPL$^{-/-}$ mice passing through HEVs in the MLN are shown (left). The y-axis indicates the ratios of the cells, which stopped more than 0.5 seconds, but detached within 10 seconds (transient arrest) or adhered more than 10 seconds (stable arrest) against total cells interacting with the vessel wall. Data represent the mean ± SD of 4 independent experiments. Representative cell interactions with MLN HEVs are shown (right). Image acquisition information is available in the supplemental Methods.

talin significantly decreased both the basal and chemokine-stimulated KIM127 epitope levels but still exhibited CXCL12-induced up-regulation of the KIM127 epitope to an extent similar to that of control cells (1.6-fold, Figure 1F; supplemental Figure 2). The effects of deletion of RAPL and talin on the KIM127 expression were similar to that of talin deletion (data not shown). On treatment with Mg^{2+} and ethyleneglycoltetraacetic acid, BAF/LFA-1/L-selectin cells depleted of Rap1, RAPL, or talin expressed the high affinity conformation of LFA-1, as evidenced by mAb24 binding,[28] and adhered to ICAM-1 (supplemental Figure 3). These results suggest that Rap1 exerts a different regulatory effect distinct from induction of the extension of LFA-1 by chemokine.

Requirement for RAPL in stable arrest of mouse lymphocytes on HEV

To further confirm whether RAPL plays an important role in stable attachment, but not during the initial arrest, we examined RAPL$^{-/-}$ T lymphocytes using the flow adhesion assay with LS12 cells expressing mouse ICAM-1. Control T cells efficiently roll on the LS12 monolayer and arrest in the presence of immobilized CCL21 (Figure 2A). This arrest was inhibited by anti–LFA-1 mAb (FD441). Although CCL21-induced transient arrest was increased, RAPL$^{-/-}$ T cells did not stably attach. The majority of RAPL$^{-/-}$ T cells were dislodged within 10 seconds at the shear stress of 2 dyne/cm^2 (Figure 2A; supplemental Videos 6-7). To confirm the

Figure 1. Requirement for Rap1, RAPL, and talin in LFA-1–mediated arrest under shear flow. (A) Knockdown of talin, RAPL, and Rap1 by shRNA. Western blots of total cell lysates from BAF/LFA-1/L-selectin cells with lentiviruses encoding control shRNA or shRNA targeting Rap1a/b-specific (Rap1KD), RAPL (RAPLKD), talin (TalinKD) are shown. Tubulin was used as a loading control. Western blots of total lysates from the double knockdown cells with lentiviruses encoding RAPL (RAPLKD) and talin (TalinKD) are also shown in the right panel. (B) Effects of anti–L-selectin, anti–LFA-1, Rap1KD, RAPLKD, TalinKD, and double KD on the interactions of BAF/LFA-1/L-selectin cells with LS12 endothelial cells. Control cells were pretreated with or without anti–L-selectin or anti–LFA-1 antibody. Then the cells perfused at 2 dyne/cm^2 on LS12 monolayers, which were immobilized with CXCL12. The digital images of interactions of BAF/LFA-1/L-selectin cells with LS12 endothelial cells were taken at 30 frames/second. The adhesive events of more than 100 cells were measured and categorized as described in the supplemental Methods. Data represent the mean ± SD of 3 independent experiments. $^*P < .001$, compared with control cells. $^{**}P < .01$, compared with RAPL or Talin KD cells. (C) Time-displacement profiles of individual cell movement over LS12 endothelial monolayers under shear flow. BAF/LFA-1/L-selectin cells were perfused at 2 dyne/cm^2 on LS12 monolayers immobilized with CXCL21. Representative profiles of the displacements over time are shown for "stable arrest" of the cells on the CXCL12 immobilized endothelium, "rolling" in the presence of anti–LFA-1 antibody (CXCL12/anti–LFA-1), "rolling" of those depleting Rap1 (CXCL12/Rap1KD), and "transient arrest" of those depleting talin (CXCL12/TalinKD) and depleting RAPL (CXCL12/RAPL). Each line represents individual cell tracking. (D) The noninteracting and rolling velocities of control BAF/LFA-1/L-selectin cell movements on LS12 in the presence of anti–L-selectin (anti–L-selectin) and anti–LFA-1 (anti–LFA-1) antibodies as well as the Rap1 knockdown cells (Rap1KD). Data represent the mean ± SD of 3 independent experiments. (E) Stopping time of control (ct), RAPLKD or talinKD, or RAPL/talin double KD BAF/LFA-1/L-selectin cells arrested on LS12 endothelial cells are shown. More than 100 cells were measured in 3 independent experiments, and representative distribution of stopping time is shown. $^*P < .02$, compared with RAPL or talin KD cells. (F) Epitope expression of mAb KIM127 on control (ct) BAF/LFA-1 cells and the Rap1 (Rap1KD), RAPL (RAPLKD), or talin (Talin KD) knockdown cells in the absence (None) or presence of CXCL12. $^*P < .05$, compared with control cells. Data are normalized for LFA-1 expression detected by TS1/18.

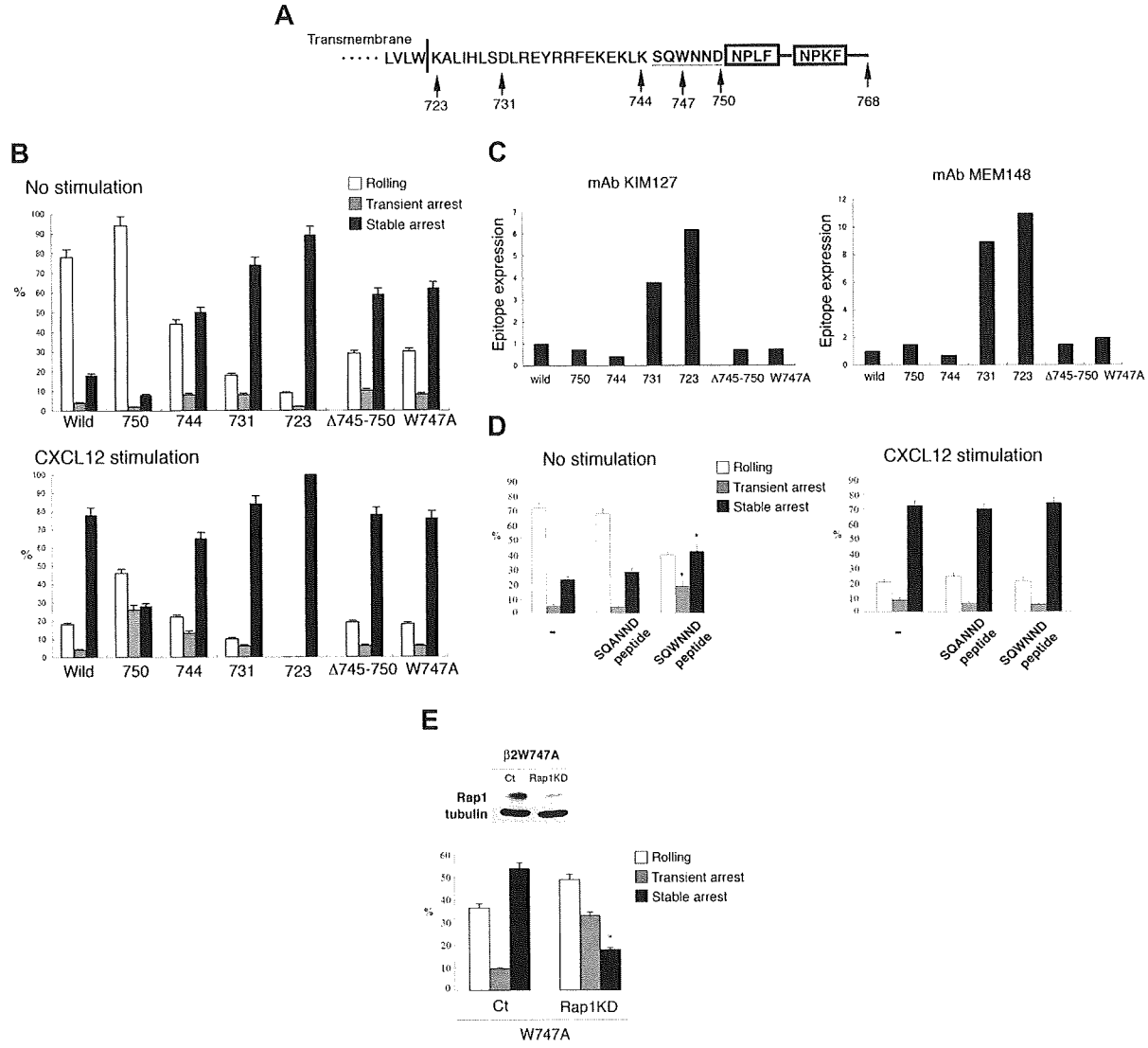

Figure 3. LFA-1 cytoplasmic regions regulate transient and stable arrest. (A) Schematic representation of the cytoplasmic region of human β2 subunit. Deletions and point mutation were made at the indicated amino acid residues. Deletion mutants include the indicated amino acids. The boxes indicate the NPXF/Y motif, which is the talin-binding region. (B) Under flow adhesion of BAF cells expressing L-selectin and LFA-1 mutants with or without CXCL12. Data represent the mean ± SD of 3 independent experiments. (C) Expression of activation epitopes detected by mAb KIM127 (left) and MEM148 (right) in unstimulated LFA-1 mutants. (D) Induction of the arrest by a penetratin-1 fusion peptide corresponding to β2/745-750. Treatment with peptide β2/745-750 (SQWNND), but not with the control peptide (SQANND; 100 μg/mL), induced the stable arrest of BAF/L-selectin/LFA-1 cells. The cells were treated with the peptides in the absence or presence of CXCL12 as described in the supplemental Methods. Data represent the mean ± SD of 3 independent experiments. $^*P < .01$, compared with the cells with control peptide. (E) Knockdown of Rap1 in BAF cells/L-selectin expressing αL/β2 W747A. (Top panel) Western blotting of vector alone (ct) or vector encoding Rap1-specific shRNA (Rap1 KD). Tubulin served as a loading control. (Bottom panel) Under flow adhesion of BAF cells/L-selectin expressing αL/β2 W747A mutation infected with lentiviruses encoding GFP alone (ct) or Rap1a/b-specific shRNA (KD). Data represent the mean ± SD of 3 independent experiments. $^*P < .005$, compared with control lymphocytes.

in vivo relevance of this result, we labeled RAPL$^{-/-}$ lymphocytes with CMTMR and injected them intravenously into normal mice and then examined lymphocyte interactions with the HEV in the mesenteric LN using intravital microscopy. Injected wild-type lymphocytes interacted with HEVs, resulting in firm attachment and subsequent accumulation of attached lymphocytes along the venules within 10 minutes (Figure 2B; supplemental Video 8). RAPL$^{-/-}$ lymphocytes appeared to tether/roll and stop normally on HEV. However, attached RAPL$^{-/-}$ lymphocytes were easily detached and accumulated poorly along the HEV (Figure 2B; supplemental Video 9). The number of stably attached cells was severely decreased, whereas the number of transiently adherent cells were not reduced (Figure 2B). These in vivo and in vitro results indicate that RAPL is not critical in the initial step of arrest but is required for subsequent adhesion stabilization.

Roles of the αL and β2 cytoplasmic domains in arrest

To identify the cytoplasmic region of LFA-1 critical for Rap1-dependent arrest, a series of deletion mutants of the β2 tail were introduced into the BAF/L-selectin cells (Figure 3A). Stable transfectants at comparable expression levels of LFA-1 (data not shown) were chosen and examined by the flow adhesion assay with LS12 cells. Carboxyl-terminal deletion of the β2 tail after amino acid 750 (Δ750) predominantly showed rolling without chemokines and decreased the chemokine-triggered stable arrest with a reciprocal increase of the transient arrest. This indicated that the region downstream of 750, containing the talin binding NPXF/Y motif, was important for stable arrest. However, the Δ750 was still capable to respond to CXCL12, indicating that the region downstream of 750 is not critical for chemokine-induced arrest. In

contrast, deletion after amino acid 744 (Δ744), 731 (Δ731), or 723 (Δ723) induced stable arrest independently of chemokines (Figure 3B). These findings suggested that the region between 745 and 750 could suppress cell arrest in the absence of activation. To examine this possibility, an internal deletion mutant lacking amino acids 745 to 750 was made. The β2Δ745-750 also induced arrest without chemokines (Figure 3B). Because tryptophan 747 is the only conserved aromatic amino acid among β integrins in this region, this W747 residue was mutated to alanine. The W747A mutation efficiently induced the stable arrest with no further augmentation by chemokines (Figure 3B; supplemental Videos 10–11). There was a slight increase of the transient arrest of Δ744 in the presence of chemokine compared with that of wild-type, implying the reduced adhesion stability of Δ744. In contrast to the β2 integrin, deletion of the αL cytoplasmic region after the GFFKR motif did not induce spontaneous arrest (supplemental Figure 4). Rather, the αLΔ1095 mutation converted the stable arrest into transient arrest with similar frequencies of the total arrest (transient plus stable), indicating that a region downstream of 1095 in αL is also critical for the stabilization of this arrest. This result is in agreement with the previous study showing that RAPL interacted with the αL cytoplasmic region.[22]

We also examined conformations of the β2 mutants showing spontaneous arrest with KIM127 β2 extension reporter mAb[29] and MEM148 open, high-affinity reporter mAb.[30] Deletion of LFA-1 after amino acids 723 and 731 (Δ723 and Δ731) led to dramatic increases in the expression of both epitopes (Figure 3C; supplemental Figure 5), indicating extended open conformations. A similar result was also obtained with the high-affinity conformation reporter mAb24 (data not shown). This result in agreement with previous studies showing that mutations in the membrane proximal region of the β subunit and the GFFKR motif of the α subunit are important to keep integrins inactive.[31,32] However, Δ744 as well as W747A mutation did not affect the expression levels of activation epitopes (Figure 3C; supplemental Figure 5), suggesting that these mutants are not the extended and open conformation of LFA-1. These results indicate that the region between 731 and 743 is sufficient for the inhibition of spontaneous extended conformations of LFA-1, and suggest that there is another critical step of the suppression of LFA-1 activation requiring the region between 745 and 755, specifically tryptophan 747.

Because the mutagenesis study suggested that the β2 cytoplasmic domain negatively regulates arrest through the region containing W747, we reasoned that similar regulation could be achieved by a trans-acting "restraint" that suppresses LFA-1 in low-affinity states by interacting with the β2/745 to 750 region. The restraint model predicts that the peptide sequence of this region can competitively inhibit interactions with a restraint resulting in stable arrest. To examine this possibility, we used the penetratin1 (P1) system. P1 fusion peptides are used as "Trojans" to efficiently deliver target peptides across the plasma membrane; and on entry into cells, the linking disulfide bond is cleaved in the cytoplasm to release the target peptide.[33] A P1 peptide linked to β2/745-750 (SQWNND) and a control peptide in which W747 was replaced with alanine (SQANND) were synthesized. When BAF/L-selectin/LFA-1 cells were treated with these peptides and infused over an LS12 monolayer, the β2/745-750 peptide but not the control peptide substantially induced transient and stable arrest without CXCL12 (Figure 3D; supplemental Videos 12-13), supporting the notion that releasing the restraint induces arrest. The peptide did not augment the arrest by CXCL12 (Figure 3D). This suggests that the intracellular peptide concentration might not be sufficient for complete release of the trans-acting restraint, or the release of restraint may not be enough for the induction of arrest. It should be noted that the treatment with the β2/745-750 peptide as well as CXCL12 did not increase the spontaneous arrest of the cells with W747A mutation (Figure 3B; supplemental Figure 6), suggesting that they might act on the same pathway by a release of the restraint in the induction of the transient arrest.

Because β2/W747A induced stable arrest as efficiently as that triggered by chemokines, we next examined the Rap1 dependency for this spontaneous arrest. Rap1 depletion by shRNA inhibited stable arrest in cells expressing β2/W747A but did not reduce transient arrest (Figure 3E); however, Rap1 depletion in cells expressing wild-type LFA-1 demonstrated rolling without arrest (Figure 1B). Taken together, these results support the notion that, although the stabilization of the nascent ligand-bound LFA-1 still requires Rap1, the W747A mutant can substitute for Rap1 function to activate LFA-1–mediated transient arrest, possibly through the release a restraint from the β2 cytoplasmic domain.

Roles of Rap1 and RAPL in cell migration over FRCs

We previously demonstrated that Rap1 and RAPL signaling induced integrin-dependent migration as well as adhesion.[34] We examined whether Rap1 and RAPL are also involved in interstitial migration after entering the LN. As a first approach to clarify the involvement of Rap1-RAPL signaling in this type of lymphocyte motility, we used the FRC cell line, BLS4, which was established from peripheral LNs and can develop ER-TR7$^+$ reticular networks in vitro.[7] BLS4 constitutively expresses VCAM-1 on the cell surface, whereas ICAM-1 is induced by TNF-α. Likewise, BLS4 cells produce CXCL12 constitutively, whereas the production of several other chemokines, including CCL4, CCL5, CCL20, and CXCL10, are augmented via TNF-α stimulation.[7] When incubated over a TNF-α–stimulated BLS4 monolayer, BAF cells exhibited polarized morphologies with a leading edge and uropod and actively migrated (Figure 4A-D). Adhesion was largely dependent on the VLA-4–VCAM-1 system because VLA-4 or VCAM-1 mAb treatment reduced adhesion levels by approximately 70% (data not shown). We then examined the contribution of Rap1 and talin. Rap1-depleted BAF cells largely retained unpolarized shapes and showed marked reduction in migration velocities and displacements, compared with those of control BAF cells (Figure 4A-B). Spa1, a Rap1GAP, suppressed cell motility more severely. The knockdown of talin did not affect cell polarization but decreased adhesion and migration of BAF/LFA-1 cells on a BLS4 monolayer (Figure 4C-D).

To address whether RAPL is also involved in lymphocyte motility on FRCs, we used T and B lymphocytes from RAPL$^{-/-}$ mice. Because primary lymphocytes show only a weak motility on BLS4 cells, T or B cells were activated with an anti-CD3 mAb or LPS for several days. In this system, wild-type T cells showed active migration with an average velocity and displacement rate of 9.5 μm/minute and 44.0 μm/10 minutes, respectively (Figure 4E-F; supplemental Video 14). Treating with mAbs for LFA-1 and VLA-4 or ICAM-1 and VCAM-1 reduced the adhesion levels of CD3-stimulated lymphoblasts by 70%, the velocity by 20% to 30%, and the displacement by 30% to 40% (data not shown). When RAPL$^{-/-}$ T cells were applied to a BLS4 monolayer, they could adhere to the monolayer, but a large fraction of them retained unpolarized shapes and migrated within a limited area with an average velocity of 5.7 μm/minute. Trajectory analysis showed that a RAPL deficiency affected movements with high velocities and displacement rates (Figure 4E-F; supplemental Video 15).

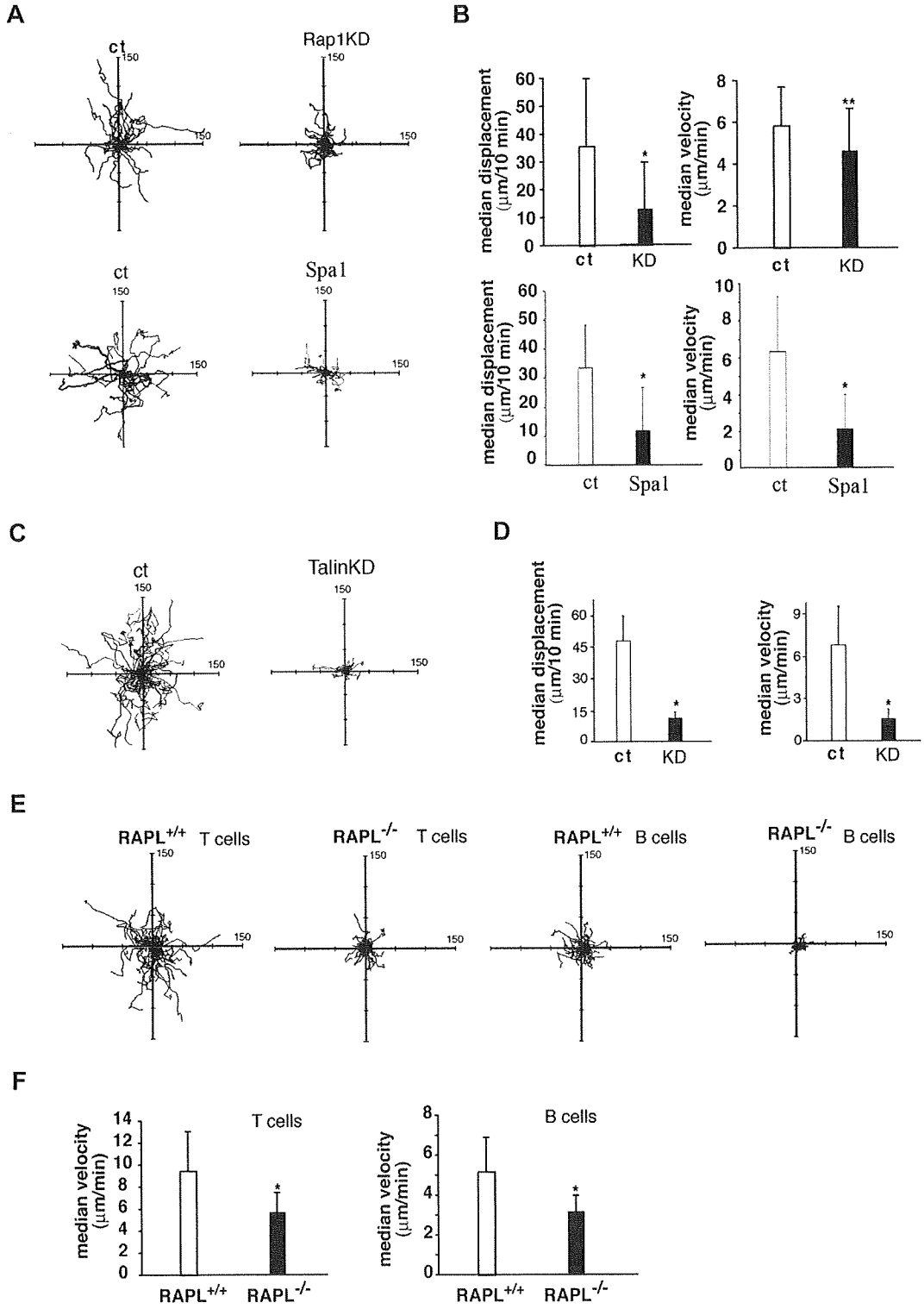

Figure 4. Cell motility over the monolayer of BLS4 cells, an ER-TR7$^+$ FRC cell line. (A) Representative cell tracks of BAF/L-selectin/LFA-1 cells transfected with vector (ct), Rap1 -specific shRNA (Rap1KD), or Spa1 over BLS4 cells. Each line represents a single-cell track. (B) Displacement and velocity of BAF/L-selectin/LFA-1 cells transfected with vector (ct, □) or Rap1-specific shRNA (KD, ■) or Spa1 (■) over BLS4 cells. Each line represents a single-cell track. *$P < .001$. **$P < .05$. (C) Representative tracks of BAF/L-selectin/LFA-1 cells transfected with vector (ct) or talin-specific shRNA (KD) over BLS4 cells. Each line represents a single-cell track. (D) Displacement and velocity of BAF/L-selectin/LFA-1 cells transfected with vector (ct, □) or Talin-specific shRNA (KD, ■) over BLS4 cells. *$P < .001$. (E) Cell motility of wild-type and RAPL$^{-/-}$ lymphocytes over the BLS4 monolayer. Representative tracks of wild-type and RAPL$^{-/-}$ T-cell blasts and B-cell blasts over BLS4 cells as indicated. Each line represents a single-cell track on the monolayer recorded every 30 seconds for 10 minutes. The median displacement was 35.1 μm/10 minutes for wild-type T cells and 10.5 μm/10 minutes for RAPL$^{-/-}$ T cells. The median displacement was 19.4 μm/10 minutes for wild-type B cells and 6.9 μm/10 minutes for RAPL$^{-/-}$ B cells. (F) Median velocity of wild-type and RAPL$^{-/-}$ T and B cells shown in panel E. The velocity data were obtained from movements measured every 30 seconds. *$P < .001$

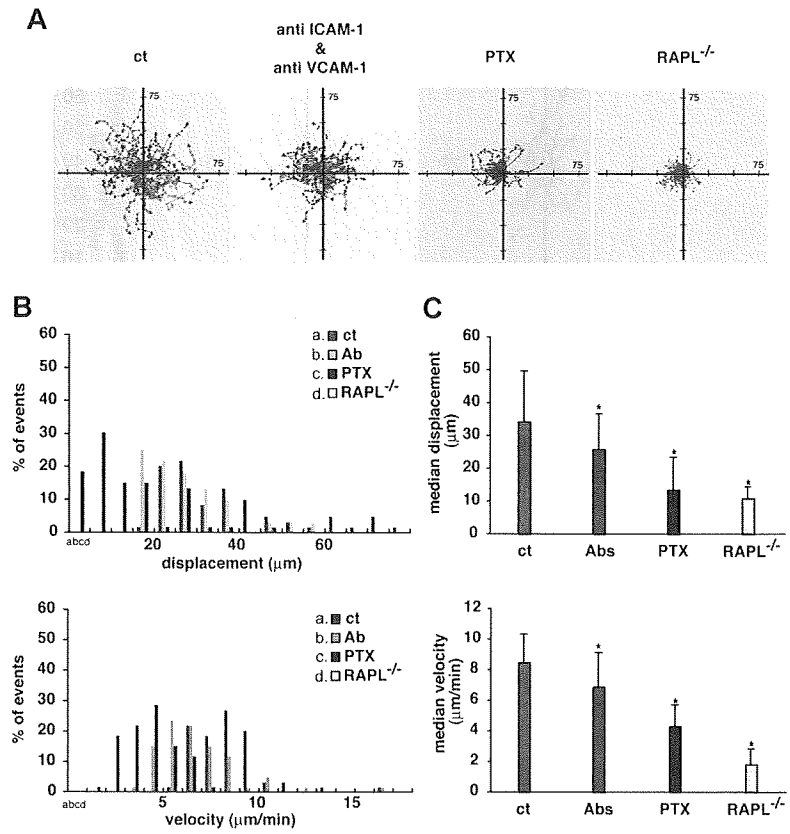

Figure 5. Contribution of Gi, integrin ligands, and RAPL to cell migration within the LN. (A) Lymphocyte movement in B-cell follicles observed by intravital microscopy of inguinal LN. Representative tracks of wild-type lymphocytes in recipient mice injected with control rat IgG (ct) (green), anti–ICAM-1 and anti–VCAM-1 mAbs (red), or pertussis toxin (blue). Representative tracks of RAPL-deficient lymphocytes (yellow) in untreated, normal recipient mice are shown. (B) Displacement and velocity profiles of wild-type and RAPL$^{-/-}$ lymphocytes in recipient mice shown in panel A. Fifty-nine cells were tracked for 10 minutes for each dataset. The velocity data were obtained from movements measured every 30 seconds. (C) Median displacement and velocity of populations shown in panel B. Statistical significance was determined by a *t* test. *$P < .001$ compared with lymphocytes in rat IgG-administered recipient mice.

RAPL$^{-/-}$ B cells migrated poorly on the BLS4 monolayer with reduced velocity and minimum displacement (Figure 4E-F). Compared with T cells, B cells exhibited slower movement on the BLS4 monolayer with a 5.2 μm/minute velocity (Figure 4E-F). These results indicate that Rap1-RAPL signaling is required for efficient directional movement of cultured lymphoblasts on the FRC monolayer through regulation of both cell polarization and integrin adhesion.

Defective interstitial migration of RAPL$^{-/-}$ lymphocytes

To further investigate whether RAPL plays an important role in interstitial migration in vivo, we recorded the movement of adoptively transferred splenic lymphocytes within the inguinal LN by intravital epifluorescence microscopy and a high-sensitivity digital CCD camera. The cortex side of the inguinal LN was exposed from the skin and set under the microscope. Preliminary experiments confirmed that this experimental setting could detect active B-cell movement in follicles but not T-cell motility in the paracortex area. Wild-type lymphocytes actively migrated with an average velocity and displacement rate of 8.5 μm/minute and 38.1 μm/10 minutes, respectively. Intraperitoneally administered anti–VCAM-1 and anti–ICAM-1 mAbs bound to the FRC and FDC networks (supplemental Figure 7) and significantly retarded movement characterized by a decreased velocity and displacement rate, whereas control rat IgG had no significant effects (Figure 5), indicating that integrin-dependent adhesion facilitates lymphocyte motility within the LN. Further, lymphocyte motility was inhibited severely by pertussis toxin treatment (Figure 5), consistent with previous reports.[35,36] Although lymphocytes were detected regardless of RAPL expression, RAPL$^{-/-}$ lymphocytes were inefficient in trafficking to the LN and required adoptive transfer of a greater numbers of lymphocytes to be tracked for 18 hours after transfer. In contrast to wild-type lymphocytes, most RAPL$^{-/-}$ lymphocytes remained near the original tracking sites with reduced average velocities (1.8 μm/minute) and displacement rates (10.9 μm/10 minutes; Figure 5). Most RAPL$^{-/-}$ lymphocytes, which either constantly changed cell shape or remained round, failed to initiate steady movement.

To examine the movement of T cells that localize primarily in the paracortical areas (100-300 μm below the capsule), intravital imaging of popliteal LN was performed using a multiphoton laser microscope 24 hours after adoptively transfer of differentially labeled wild-type and RAPL$^{-/-}$ T cells into the same recipient mice. RAPL$^{-/-}$ T cells exhibited a significant reduction in mean velocity compared with wild-type T cells. Trajectory analysis indicated that the 3-dimensional displacement of RAPL$^{-/-}$ T cells during the observation period was severely compromised (Figure 6; supplemental Video 16). Consistent with this observation, RAPL-deficient lymphocytes were distributed in limited areas within the LN compared with wild-type lymphocytes after adoptive transfer (data not shown). Collectively, these results reveal that RAPL contributes to efficient interstitial migration.

Discussion

This study provides novel information on the roles of Rap1 and RAPL signaling during entry into and trafficking within the LN. Rap1 is necessary for the rapid, chemokine-induced activation of LFA-1 that mediates arrest, but RAPL is not involved in the Rap1-dependent initial step of this arrest. Subsequently, Rap1, together with RAPL, stabilizes adhesion. They are also required for the motility of cultured lymphoblasts on FRC cells in vitro and contribute to the high-velocity directional movements of primary

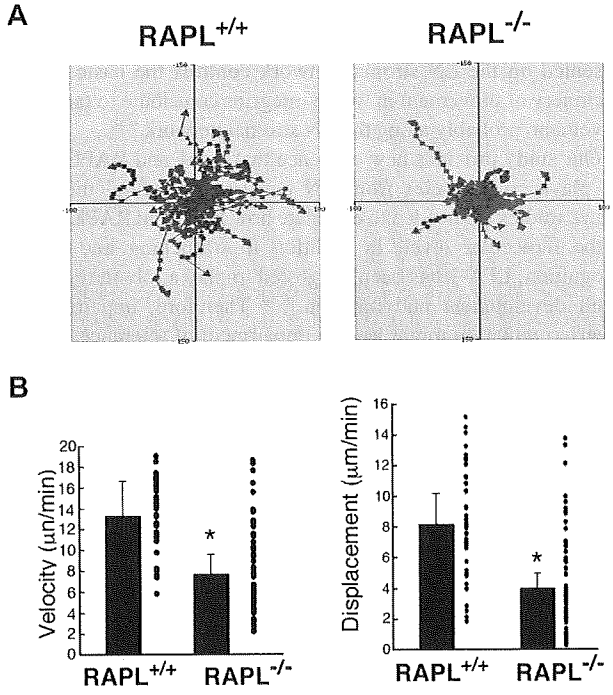

Figure 6. Interstitial migration of wild-type and RAPL-deficient T cells analyzed by intravital 2-photon microscopy. (A) Representative tracks of wild-type T cells (red) and RAPL$^{-/-}$ T cells (green) in popliteal LN. Each line represents a single T-cell track. (B) Displacement and velocity profiles of wild-type T cells and RAPL-deficient T cells. Forty cells of each type were tracked for 30 minutes for each dataset. *$P < .001$, compared with wild-type cells.

T and B cells mediated, at least in part, by ICAM-1 and VCAM-1 within the LN.

Because LFA-1 can act as the rolling receptor in some cellular contexts and under low shear flow, allowing pre-engagement of LFA-1 before the arrest,[6,26] it is difficult to distinguish intracellular signaling required for the initial arrest from the subsequent stabilization of engaged LFA-1. We confirmed that, in our experimental system reproducing L-selectin–dependent rolling to arrest by LFA-1 under shear flow at 2 dyne/cm^2, the blockade of LFA-1 or ICAM-1 did not affect rolling frequencies and velocities, ruling out the possibility of the pre-engagement of LFA-1 before the arrest. Under this condition, it is predicted that, when inside-out signaling by chemokines is blocked, the cells keep rolling through L-selectin engagement, whereas inhibition of the outside-in signaling should result in unstable arrest by LFA-1. The experiments with shRNA-mediated knockdown demonstrate that Rap1 acts through inside-out signaling and RAPL through outside-in signaling during arrest. This raises an issue as to how Rap1 possibly regulates subsecond activation independently of RAPL. There are other Rap1-binding proteins potentially involved in lymphocyte adhesion, including RIAM.[37] However, CCL25-triggered adhesion of a human T-cell line to VCAM-1 through VLA-4 was inhibited by knockdown of Rap1a/b and RAPL, but not RIAM.[38] Therefore, it is an important issue to be solved in the future, as to the mechanism by which Rap1 regulates subsecond LFA-1 activation.

The W747A mutation of the cytoplasmic region of the β2 tail induced spontaneous arrest independent of chemokines. It is widely thought that the association (clasping) and separation (unclasping) of the α and β tail is translated into inactive, bent low-affinity conformations and active, extended high-affinity conformations, respectively, and that the inside-out and outside-in signaling induces the separation.[2] The mutational and structural studies have demonstrated that the membrane proximal "hinge" region, GFFKR" in the α and the corresponding β cytoplasmic region, plays a critical role for clasping and restraining the integrin in a resting state.[31,32] Therefore, it is possible that the W747A mutation causes unclasping, leading to constitutive activation of LFA-1. This is doubtful for several reasons. First, W747 is far from the hinge region (corresponding to β2 723-731), and the tryptophan residue at the homologous position in $\alpha_{IIb}\beta_3$ is not involved in the α and β cytoplasmic tail contacts.[39] Second, deletion after the GFFKR motif did not result in constitutive activation. Finally, the W747 mutation did not induce extended, open conformations of LFA-1, which are induced by hinge-disrupting mutations, such as Δ723 and Δ731 mutations in this study. Thus, the chemokine-independent arrest by the W747A mutation is not simply explained by unclasping of the αL and β2 subunit. Because the β2/745-750 region overlaps the talin interacting region,[40] talin might act as a restraint as well as a positive regulator.[41] However, knockdown of talin1, the major isotype expressed in splenic lymphocytes and BAF cells, with talin2 below detectable levels (data not shown), failed to increase arrest adhesion without chemokine but severely inhibited stable arrest, thus indicating that talin does not act as restraint but plays the important role in stable adhesion.[27,42] There has been so far no reports of β integrin-associated molecules interacting with the W747 residue. Immunoprecipitation experiments are so far unsuccessful to detect the putative restraint. Further studies with improved methods are needed to clarify the molecular characterization of restraint.

The result showing that the short peptide (S745-D750) covering the critical W747 induced the spontaneous arrest suggests that a trans-acting "restraint" binds to this region, keeping LFA-1 inactive, and release of the restraint by competitive inhibition with the peptide could lead to activation of LFA-1 for the initial arrest. It is conceivable that Rap1 could release the restraint on chemokine stimulation and induce the initial arrest because the knockdown of Rap1 in W747A mutants did not abrogate transient arrest (Figure 3). We could not clarify what effect a release of the restraint has on LFA-1. Previous studies suggest that LFA-1 extension with intermediate to high affinities induces arrest under shear flow,[6,26,27] and in human T cells LFA-1 unbending by chemokine was suppressed by inhibition of Rap1 activation. However, chemokine-triggered LFA-1 extension did not require Rap1 in our system, suggesting other compensatory mechanisms through Rap1-related GTPases, such as Rap2, or through Rho-PI5kinase,[43] operating for LFA-1 extension in a cellular context-dependent manner. Our results suggest that the function of Rap1 in the initial arrest occurs independently of extension conformational changes; instead, chemokine signaling coordinates the Rap1 and Rho signaling to initiate arrest.

Our results showed that RAPL and talin acted at the stabilization step but did not play a critical role in initial arrest. We previously showed that RAPL could associate with LFA-1 depending on activated Rap1 and the αL cytoplasmic tail, which was necessary for binding to ICAM-1.[22] We could not detect the association of RAPL and talin, suggesting that they act independently through binding the αL and β2 tail, respectively. The arrest of cells expressing β2/W747A or Δ745-750 also required RAPL and talin for stabilization (data not shown). Further, knockdown of Rap1 converts stable arrest into transient arrest in W747A mutants, indicating that stabilization of ligand-engaged LFA-1 still requires Rap1. Because Rap1 is also activated by ligand-bound LFA-1 in lymphocytes,[44] sequential Rap1 activation might occur by chemokine and ligand-bound LFA-1 to stabilize the arrest through RAPL, together with talin. Based on these findings, we propose sequential

Rap1-mediated regulatory steps that control arrest and firm adhesion (supplemental Figure 8). LFA-1 is kept in a low-affinity bent-conformation state by the binding of a restraint to the β2 tail. Rap1 activation by chemokine initiates the adhesion cascade by release of the restraint, which could induce subsecond arrest adhesion (step 1). Transient adhesion is stabilized through the continuing activity of Rap1 by the binding of talin or other β2 tail interactors and RAPL (step 2), perhaps through separation of cytoplasmic tails.[5] In addition, shear force facilitates affinity conformation of the I domain and enforced stabilized ligand-bound extended conformation.[27] Thus, our results support a model that arrest adhesion is regulated by bidirectional, inside-out and outside-in signaling,[45] and Rap1 activation is required throughout these processes.

Rap1 and RAPL function uniquely to induce migratory cell shapes and facilitate cell migration through endothelial cells under shear flow or on ICAM-1–coated surfaces.[23,34,46] However, whether this signaling also plays a role in dynamic lymphocyte interstitial migration in lymphoid tissues is not yet known. Lymphoblasts exhibited active migration in vitro, as seen on the BLS4 FRC monolayer in this study. This motility was mediated mostly by LFA-1 and VLA-4 and severely impaired by Rap1 inhibition. The inhibitory effect of Rap1 depletion was also confirmed by Rap1 inhibition by Spa1. The inhibitory levels by Spa1 were more evident than Rap1 depletion. This suggests that the weak adhesive interactions resulting from incomplete Rap1 depletion can still support cell migration under nonflow conditions, or other signaling pathways could be involved in cell motility. RAPL$^{-/-}$ T and B lymphoblasts exhibited reduced motility and displacement with poor development of cell polarity. In vivo, primary RAPL$^{-/-}$ lymphocytes remained motile, to some extent, in the B-cell follicle and T-cell areas. However, they changed orientation frequently with reduced average velocities, resulting in defective long-distance migration. We showed that administering ICAM-1 and VCAM-1 antibodies in vivo decreased only high-velocity directional movements of lymphocytes. A small reduction in average velocity was also observed by CD18$^{-/-}$ lymphocytes.[10] Nevertheless, the contribution of integrins to overall cell motility is relatively small compared with that of Gi signaling and RAPL, suggesting that other adhesion molecules and/or immobilized chemokines by themselves[10,47] support cell motility in the LN environment. This implies that Rap1 and RAPL play more fundamental roles in cell motility in addition to integrin regulation. For example, chemokines stimulate lymphocyte polarization with a leading edge and uropod, a process that is independent of cell attachment but requires Rap1 and RAPL.[22,34] Thus, Gi signaling followed by Rap1 and RAPL triggered by homeostatic chemokines presented on the LN stromal network controls the basic cellular machinery of movement in which integrins contribute to fast-speed movement, probably along the LN stromal network.[9,10]

Our study provides new evidence that Rap1 and RAPL signaling plays critical roles from LN entry to interstitial migration. Future studies are needed to elucidate how Rap1 and RAPL operate at the molecular level. In addition to trafficking and antigen recognition, LFA-1 has been suggested to play a role in regulatory T-cell development and function.[48,49] Therefore, impairment of integrin regulation might lead to impairment of tolerance, leading to autoimmunity. The effects of Rap1 and RAPL on homeostasis of the immune system need detailed analysis.

Acknowledgments

The authors thank Ms R. Hamaguchi for technical assistance and Dr N. O'Reilly for peptide synthesis.

This work was supported in part by the Ministry of Education, Culture, Sports, Science and Technology of Japan (grant-in-aid), the Toray Science Foundation, and the Naito Foundation.

Authorship

Contribution: Y.E. and K.K. performed the experiments, analyzed the data, and wrote some parts of the paper; T. Katakai and Y.U. performed some parts of the experiments; T.N., H.I., J.N., and T.O. supported the experiments using 2-photon microscopy; R.K. provided essential reagents; T.T. and M.M. supported the observation of lymphocyte interaction with HEV by intravital microscopy; N.H. provided essential reagents, discussed the results, and edited the paper; and T. Kinashi designed and supported the project and wrote the paper.

Conflict-of-interest disclosure: The authors declare no competing financial interests.

The current affiliation for K.K. is Laboratory of Immunology, Department of Life Science, School of Science and Technology, Kwanseigakuin University, Osaka, Japan.

Correspondence: Tatsuo Kinashi, Department of Molecular Genetics, Institute of Biomedical Science, Kansai Medical University, Fumizono-cho 10-15, Moriguch, Osaka, 570-8506, Japan; e-mail: kinashi@takii.kmu.ac.jp.

References

1. Hynes RO. Integrins: versatility, modulation, and signaling in cell adhesion. *Cell.* 1992;69(1):11-25.
2. Carman CV, Springer TA. Integrin avidity regulation: are changes in affinity and conformation underemphasized? *Curr Opin Cell Biol.* 2003;15(5):547-556.
3. Hynes RO. Integrins: bidirectional, allosteric signalling machines. *Cell.* 2002;110(6):673-687.
4. Butcher EC, Picker LJ. Lymphocyte homing and homeostasis. *Science.* 1996;272(5258):60-66.
5. Kim M, Carman CV, Springer TA. Bidirectional transmembrane signaling by cytoplasmic domain separation in integrins. *Science.* 2003;301(5640):1720-1725.
6. Salas A, Shimaoka M, Kogan AN, Harwood C, von Andrian UH, Springer TA. Rolling adhesion through an extended conformation of integrin alphaLbeta2 and relation to alpha I and beta I-like domain interaction. *Immunity.* 2004;20(4):393-406.
7. Katakai T, Hara T, Sugai M, Gonda H, Shimizu A. Lymph node fibroblastic reticular cells construct the stromal reticulum via contact with lymphocytes. *J Exp Med.* 2004;200(6):783-795.
8. Sumen C, Mempel TR, Mazo IB, von Andrian UH. Intravital microscopy: visualizing immunity in context. *Immunity.* 2004;21(3):315-329.
9. Bajénoff M, Egen JG, Koo LY, et al. Stromal cell networks regulate lymphocyte entry, migration, and territoriality in lymph nodes. *Immunity.* 2006;25(6):989-1001.
10. Woolf E, Grigorova I, Sagiv A, et al. Lymph node chemokines promote sustained T lymphocyte motility without triggering stable integrin adhesiveness in the absence of shear forces. *Nat Immunol.* 2007;8(10):1076-1085.
11. Fukui Y, Hashimoto O, Sanui T, et al. Haematopoietic cell-specific CDM family protein DOCK2 is essential for lymphocyte migration. *Nature.* 2001;412(6849):826-831.
12. Nombela-Arrieta C, Mempel TR, Soriano SF, et al. A central role for DOCK2 during interstitial lymphocyte motility and sphingosine-1-phosphate-mediated egress. *J Exp Med.* 2007;204(3):497-510.
13. Bos JL, de Rooij J, Reedquist KA. Rap1 signaling: adhering to new models. *Nat Rev Mol Cell Biol.* 2001;2(5):369-377.
14. Kinashi T, Katagiri K. Regulation of immune cell adhesion and migration by regulator of adhesion and cell polarization enriched in lymphoid tissues. *Immunology.* 2005;116(2):164-171.
15. Chrzanowska-Wodnicka M, Smyth SS, Schoenwaelder SM, Fischer TH, White GC 2nd. Rap1b is required for normal platelet function and

hemostasis in mice. *J Clin Invest.* 2005;115(3):680-687.

16. Duchniewicz M, Zemojtel T, Kolanczyk M, Grossmann S, Scheele JS, Zwartkruis FJ. Rap1A-deficient T and B cells show impaired integrin-mediated cell adhesion. *Mol Cell Biol.* 2006;26(2):643-653.
17. Li Y, Yan J, De P, et al. Rap1a null mice have altered myeloid cell functions suggesting distinct roles for the closely related Rap1a and 1b proteins. *J Immunol.* 2007;179(12):8322-8331.
18. Chu H, Awasthi A, White GC 2nd, Chrzanowska-Wodnicka M, Malarkannan S. Rap1b regulates B cell development, homing, and T cell-dependent humoral immunity. *J Immunol.* 2008;181(5):3373-3383.
19. Bergmeier W, Goerge T, Wang HW, et al. Mice lacking the signaling molecule CalDAG-GEFI represent a model for leukocyte adhesion deficiency type III. *J Clin Invest.* 2007;117(6):1699-1707.
20. Pasvolsky R, Feigelson SW, Kilic SS, et al. A LAD-III syndrome is associated with defective expression of the Rap-1 activator CalDAG-GEFI in lymphocytes, neutrophils, and platelets. *J Exp Med.* 2007;204(7):1571-1582.
21. Ghandour H, Cullere X, Alvarez A, Luscinskas FW, Mayadas TN. Essential role for Rap1 GTPase and its guanine exchange factor CalDAG-GEFI in LFA-1 but not VLA-4 integrin mediated human T-cell adhesion. *Blood.* 2007;110(10):3682-3690.
22. Katagiri K, Maeda A, Shimonaka M, Kinashi T. RAPL, a Rap1-binding molecule that mediates Rap1-induced adhesion through spatial regulation of LFA-1. *Nat Immunol.* 2003;4(8):741-748.
23. Katagiri K, Ohnishi N, Kabashima K, et al. Crucial functions of the Rap1 effector molecule RAPL in lymphocyte and dendritic cell trafficking. *Nat Immunol.* 2004;5(10):1045-1051.
24. Kimura N, Mitsuoka C, Kanamori A, et al. Reconstitution of functional L-selectin ligands on a cultured human endothelial cell line by cotransfection of alpha1→3 fucosyltransferase VII and newly cloned GlcNAcbeta:6-sulfotransferase cDNA. *Proc Natl Acad Sci U S A.* 1999;96(8):4530-4535.
25. Finger EB, Puri KD, Alon R, Lawrence MB, von Andrian UH, Springer TA. Adhesion through L-selectin requires a threshold hydrodynamic shear. *Nature.* 1996;379(6562):266-269.
26. Salas A, Shimaoka M, Phan U, Kim M, Springer TA. Transition from rolling to firm adhesion can be mimicked by extension of integrin alphaLbeta2 in an intermediate affinity state. *J Biol Chem.* 2006;281(16):10876-10882.
27. Shamri R, Grabovsky V, Gauguet JM, et al. Lymphocyte arrest requires instantaneous induction of an extended LFA-1 conformation mediated by endothelium-bound chemokines. *Nat Immunol.* 2005;6(5):497-506.
28. Dransfield I, Hogg N. Regulated expression of Mg2+ binding epitope on leukocyte integrin alpha subunits. *EMBO J.* 1989;8(12):3759-3765.
29. Lu C, Shimaoka M, Zang Q, Takagi J, Springer TA. Locking in alternate conformations of the integrin αLβ2 I domain with disulfide bonds reveals functional relationships among integrin domains. *Proc Natl Acad Sci U S A.* 2001;98(5):2393-2398.
30. Tang RH, Tng E, Law SK, Tan SM. Epitope mapping of monoclonal antibody to integrin αL β2 hybrid domain suggests different requirements of affinity states for intercellular adhesion molecules (ICAM)-1 and ICAM-3 binding. *J Biol Chem.* 2005;280(32):29208-29216.
31. Hughes PE, Diaz-Gonzalez F, Leong L, et al. Breaking the integrin hinge: a defined structural constraint regulates integrin signaling. *J Biol Chem.* 1996;271(12):6571-6574.
32. Lu CF, Springer TA. The alpha subunit cytoplasmic domain regulates the assembly and adhesiveness of integrin lymphocyte function-associated antigen-1. *J Immunol.* 1997;159(1):268-278.
33. Derossi D, Chassaing G, Prochiantz A. Trojan peptides: the penetratin system for intracellular delivery. *Trends Cell Biol.* 1998;8(2):84-87.
34. Shimonaka M, Katagiri K, Nakayama T, et al. Rap1 translates chemokine signals to integrin activation, cell polarization, and motility across vascular endothelium under flow. *J Cell Biol.* 2003;161(2):417-427.
35. Okada T, Cyster JG. CC chemokine receptor 7 contributes to Gi-dependent T cell motility in the lymph node. *J Immunol.* 2007;178(5):2973-2978.
36. Han SB, Moratz C, Huang NN, et al. Rgs1 and Gnai2 regulate the entrance of B lymphocytes into lymph nodes and B cell motility within lymph node follicles. *Immunity.* 2005;22(3):343-354.
37. Lafuente EM, van Puijenbroek AA, Krause M, et al. RIAM, an Ena/VASP and Profilin ligand, interacts with Rap1-GTP and mediates Rap1-induced adhesion. *Dev Cell.* 2004;7(4):585-595.
38. Parmo-Cabañas M, Garcia-Bernal D, Garcia-Verdugo R, Kremer L, Marquez G, Teixido J. Intracellular signaling required for CCL25-stimulated T cell adhesion mediated by the integrin alpha4beta1. *J Leukoc Biol.* 2007;82(2):380-391.
39. Vinogradova O, Velyvis A, Velyviene A, et al. A structural mechanism of integrin alpha(IIb)beta(3) "inside-out" activation as regulated by its cytoplasmic face. *Cell.* 2002;110(5):587-597.
40. Wegener KL, Partridge AW, Han J, et al. Structural basis of integrin activation by talin. *Cell.* 2007;128(1):171-182.
41. Tadokoro S, Shattil SJ, Eto K, et al. Talin binding to integrin beta tails: a final common step in integrin activation. *Science.* 2003;302(5642):103-106.
42. Smith A, Carrasco YR, Stanley P, Kieffer N, Batista FD, Hogg N. A talin-dependent LFA-1 focal zone is formed by rapidly migrating T lymphocytes. *J Cell Biol.* 2005;170(1):141-151.
43. Bolomini-Vittori M, Montresor A, Giagulli C, et al. Regulation of conformer-specific activation of the integrin LFA-1 by a chemokine-triggered Rho signaling module. *Nat Immunol.* 2009;10(2):185-194.
44. Lin KB, Freeman SA, Zabetian S, et al. The rap GTPases regulate B cell morphology, immune-synapse formation, and signaling by particulate B cell receptor ligands. *Immunity.* 2008;28(1):75-87.
45. Alon R, Dustin ML. Force as a facilitator of integrin conformational changes during leukocyte arrest on blood vessels and antigen-presenting cells. *Immunity.* 2007;26(1):17-27.
46. Miertzschke M, Stanley P, Bunney TD, Rodrigues-Lima F, Hogg N, Katan M. Characterization of interactions of adapter protein RAPL/Nore1B with RAP GTPases and their role in T cell migration. *J Biol Chem.* 2007;282(42):30629-30642.
47. Lämmermann T, Bader BL, Monkley SJ, et al. Rapid leukocyte migration by integrin-independent flowing and squeezing. *Nature.* 2008;453(7191):51-55.
48. Marski M, Kandula S, Turner JR, Abraham C. CD18 is required for optimal development and function of CD4+CD25+ T regulatory cells. *J Immunol.* 2005;175(12):7889-7897.
49. Onishi Y, Fehervari Z, Yamaguchi T, Sakaguchi S. Foxp3+ natural regulatory T cells preferentially form aggregates on dendritic cells in vitro and actively inhibit their maturation. *Proc Natl Acad Sci U S A.* 2008;105(29):10113-10118.

The EMBO Journal (2009), 1–13 | © 2009 European Molecular Biology Organization | All Rights Reserved 0261-4189/09
www.embojournal.org

THE EMBO JOURNAL

Mst1 controls lymphocyte trafficking and interstitial motility within lymph nodes

Koko Katagiri[1], Tomoya Katakai[1], Yukihiko Ebisuno[1], Yoshihiro Ueda[1], Takaharu Okada[2,3] and Tatsuo Kinashi[1,*]

[1]Department of Molecular Genetics, Kansai Medical University, Fumizono-cho, Moriguchi-City, Osaka, Japan, [2]Department of Synthetic Chemistry and Biological Chemistry, Innovative Techno-Hub for Integrated Medical Bio-imaging, Graduate School of Engineering, Kyoto University, Katsura Campus, Nishikyo-ku, Kyoto, Japan and [3]Research Unit for Immunodynamics, RIKEN, Research Center for Allergy and Immunology, Suehiro-cho, Tsurumi-ku, Yokohama, Kanagawa, Japan

The regulation of lymphocyte adhesion and migration plays crucial roles in lymphocyte trafficking during immunosurveillance. However, our understanding of the intracellular signalling that regulates these processes is still limited. Here, we show that the Ste20-like kinase Mst1 plays crucial roles in lymphocyte trafficking *in vivo*. Mst1$^{-/-}$ lymphocytes exhibited an impairment of firm adhesion to high endothelial venules, resulting in an inefficient homing capacity. *In vitro* lymphocyte adhesion cascade assays under physiological shear flow revealed that the stopping time of Mst1$^{-/-}$ lymphocytes on endothelium was markedly reduced, whereas their L-selectin-dependent rolling/tethering and transition to LFA-1-mediated arrest were not affected. Mst1$^{-/-}$ lymphocytes were also defective in the stabilization of adhesion through α4 integrins. Consequently, Mst1$^{-/-}$ mice had hypotrophic peripheral lymphoid tissues and reduced marginal zone B cells and dendritic cells in the spleen, and defective emigration of single positive thymocytes. Furthermore, Mst1$^{-/-}$ lymphocytes had impaired motility over lymph node-derived stromal cells and within lymph nodes. Thus, our data indicate that Mst1 is a key enzyme involved in lymphocyte entry and interstitial migration.

The EMBO Journal advance online publication, 2 April 2009; doi:10.1038/emboj.2009.82
Subject Categories: cell & tissue architecture; immunology
Keywords: adhesion; LFA-1; migration; Mst1

Introduction

Naive lymphocytes continuously circulate between secondary lymphoid tissues and vasculatures in search of foreign antigens (Butcher *et al*, 1999). Lymphocyte trafficking in the peripheral lymph nodes (LNs) is generally divided into four steps: entry through the high endothelial venules (HEV), interstitial migration, antigen scanning and exit through the efferent lymphatics (von Andrian and Mempel, 2003). Our understanding of the lymphocyte trafficking has been greatly advanced by the identification of adhesion molecules, chemokines, phospholipids and their receptors. During lymphocyte homing to the peripheral LN, naive lymphocytes are first captured by weak binding between L-selectin and a sulphated sialyl Le^x-related carbohydrate, resulting in rolling on the HEV. When rolling lymphocytes are exposed to chemokines on the luminal side of the HEV, chemokine signalling coupled with Gi hetero-trimeric G proteins activates LFA-1, resulting in a complete stop. In gut-associated lymphoid tissues, α4β7 and mucosal addressin cell adhesion molecule-1 (MAdCAM-1) also support lymphocyte rolling and arrest. Within seconds to minutes, lymphocyte adhesion is stabilized and these cells transmigrate through the HEV into the tissues. Recent observations using multiphoton microscopy have revealed a robust random walk-like motility of naive lymphocytes within the LNs (Sumen *et al*, 2004). Lymphocytes appear to move in close proximity to intricate stromal networks composed of fibroblastic reticular cells in the paracortex and follicular dendritic cells (DCs) in the follicles (Bajenoff *et al*, 2006), suggesting that cell–cell interactions and/or tissue-derived factors enhance cell motility.

Chemokines, in either gradients or nongradients, can activate integrins and induce lymphocyte polarized morphology, generating a leading edge and uropod and stimulating cell motility (Sanchez-Madrid and del Pozo, 1999; Stachowiak *et al*, 2006). Chemokine signalling is coupled with pertussis toxin-sensitive Gi/o hetero-trimeric G proteins, as illustrated by the ability of pertussis toxin treatment to inhibit chemokine-triggered integrin activation and attachment to the HEV (Butcher *et al*, 1999) as well as lymphocyte motility within the LN (Okada and Cyster, 2007). Gene targeting of Gαi2 impairs B-cell lymphocyte homing and interstitial motility (Han *et al*, 2005). Chemokines activate multiple signalling pathways, including the Ras/Rho family of small GTPases. For example, DOCK2 is a Rac guanine exchange factor that is critical for actin cytoskeletal rearrangements in lymphocytes (Fukui *et al*, 2001), integrin activation and trafficking in B cells (Nombela-Arrieta *et al*, 2004), and directional high-velocity lymphocyte movement within the LN (Nombela-Arrieta *et al*, 2007). Rho GTPase signalling also plays important roles in lymphocyte adhesion and migration (Laudanna *et al*, 2002). Indeed, the actin-nucleating and polymerization protein, mDia1, acts as a downstream Rho GTPase effector and is required for efficient chemokine-stimulated actin polymerization and T-cell trafficking *in vivo* (Sakata *et al*, 2007). Coronin1, an Arp2/3 inhibitory protein, is required for efficient T-cell trafficking *in vivo*, uropod formation and cell survival (Foger *et al*, 2006).

In addition to actin regulators, the Rap1 small GTPase activates integrins and stimulates lymphocyte polarization and motility (Bos *et al*, 2001; Kinashi, 2005). A deficiency in the Rap1-specific CalDAG-GEFI through gene targeting in

*Corresponding author. Department of Molecular Genetics, Kansai Medical University, Fumizono-cho 10-15, Moriguchi-City, Osaka, 570-8506, Japan. Tel.: +81 6 6993 9445; Fax: +81 6 6994 6099; E-mail: kinashi@takii.kmu.ac.jp

Received: 4 December 2008; accepted: 3 March 2009

mice (Crittenden *et al*, 2004; Bergmeier *et al*, 2007) or abnormal splicing in human LAD-III patients (Pasvolsky *et al*, 2007), severely impairs the functions of leukocyte and platelet integrins. We reported earlier that RAPL (also known as RASSF5b), a Rap1-GTP binding protein expressed predominantly in lymphoid tissues, was required for lymphocyte adhesion through LFA-1 and α4 integrins and cell polarization triggered by chemokines. RAPL$^{-/-}$ lymphocytes showed defective lymphocyte homing to peripheral LN (Katagiri *et al*, 2003, 2004). We identified mammalian Ste20-like kinase (Mst1, also known as Stk4) as a critical RAPL effector. RAPL associates with Mst1 and regulates the localization and kinase activity of Mst1. Knockdown of Mst1 showed that it is required for polarized morphology and integrin-dependent lymphocyte adhesion (Katagiri *et al*, 2006).

Mst1 was originally identified as a protein kinase homologous to yeast sterile 20 that acts downstream of the pheromone-linked G protein in the mating pathway (Creasy and Chernoff, 1995). The mammalian Ste20 group of kinases regulates diverse biological functions including proliferation, differentiation, apoptosis, morphogenesis and cytoskeletal rearrangement. Mst1 was reported earlier to be involved in apoptosis through caspase-mediated proteolytic activation and histone H2B phosphorylation (Cheung *et al*, 2003), or in a proapoptotic pathway of Ki-Ras through Nore1 (Khokhlatchev *et al*, 2002). Hippo, the *Drosophila* ortholog of mammalian Mst1 and Mst2, has been shown to be involved in cell contact inhibition and the determination of organ size through negative regulation of cell proliferation and apoptosis (Zeng and Hong, 2008). To clarify the physiological roles of Mst1 in primary lymphocytes and trafficking *in vivo*, we generated Mst1-deficient mice. Mst1-deficient mice grew normally with no gross abnormalities. However, peripheral lymphoid organs were hypoplastic. Mst1$^{-/-}$ lymphocyte trafficking to the peripheral LN was defective due to impairment at a transition from transient arrest to stable attachment of lymphocytes on HEV. Furthermore, Mst1$^{-/-}$ lymphocytes exhibited defective motility on LN-derived stromal cells and interstitial migration within LNs. Our study also reveals that Mst1 is required for proper localization of marginal zone B (MZB) cells and splenic CD11c^{+} DC. Thus, these results show the crucial roles of Mst1 in regulating lymphocyte trafficking.

Results

Hypoplastic secondary lymphoid organs in Mst1$^{-/-}$ mice

The Mst1 protein was expressed predominantly in lymphoid tissues, and both T and B cells expressed Mst1. Mst1 was also detected at lower levels in the lung and brain but was below detectable levels in the kidney, liver, heart and skeletal muscle (Figure 1A). To generate Mst1$^{-/-}$ mice, mice carrying floxed Mst1 alleles (Mst1$^{f/f}$) were produced by gene targeting, in which exon 1 containing the initiation codon was flanked with loxP sites, and then mated with CAG-Cre transgenic mice to delete exon 1 ubiquitously (Supplementary Figure 1). Southern blot analysis confirmed that exon 1 was completely deleted in Cre^{+} Mst1$^{f/f}$ mice (Supplementary Figure 1). Although Mst1 was comparably expressed in wild-type and Mst1$^{f/f}$ mice, the Mst1 protein was not detected in the tissues of Cre^{+} Mst1$^{f/f}$ mice with no apparent generation of a truncated Mst1 protein (Figure 1A). We hereafter refer to Cre^{+} Mst1$^{f/f}$ mice as Mst1$^{-/-}$ mice. Mst2, which is homologous to Mst1 (78% amino acid identity), was expressed in all tissues examined, and there were no concomitant changes in expression with the Mst1 deficiency (Figure 1A). Mst1$^{-/-}$ mice were born with expected Mendelian frequencies and grew normally without gross abnormalities. Analysis of Mst1$^{-/-}$ tissues revealed hypoplastic lymphoid tissues, whereas there were no apparent abnormalities in other tissues including the lung and brain (data not shown). The number of both T and B cells was decreased in the peripheral LN, Peyer's patches and spleen (Figure 1B, D and F). Immunohistology showed decreases in the sizes and cellular densities of B-cell follicles and T-cell areas of these secondary lymphoid tissues (Figure 1C, E and G). The architecture of lymphoid tissues, including the segregation of T and B cells, distribution of the HEV, and stromal networks appeared normal (Figure 1; Supplementary Figure 2). The proliferative response of Mst1$^{-/-}$ B cells stimulated with BCR ligation was normal, whereas T-cell growth responses were rather augmented compared with control cells when stimulated with TCR ligation (Supplementary Figure 3). There were no significant differences in spontaneous apoptosis of mature T and B cells, although double-positive thymocytes from Mst1$^{-/-}$ mice displayed slightly enhanced cell survival (see below). Therefore, proliferation and apoptosis could not account for the reduced lymphocyte numbers in lymphoid tissues.

Defective lymphocyte trafficking to the peripheral LN

As the cellularity in peripheral lymphoid tissues was reduced, we examined whether an Mst1 deficiency could impair lymphocyte homing to secondary lymphoid organs. T and B lymphocytes were isolated from the LNs and spleens of Mst1$^{f/f}$ and Mst1$^{-/-}$ mice, both of which exhibited naive phenotypes for T cells (CD62L^{hi}CD44^{lo}CD69^{-}) and B cells (CD62 L^{+}IgM^{+}IgD^{hi}). Control Mst1$^{f/f}$ and Mst1$^{-/-}$ lymphocytes were differentially labelled and adoptively transferred into normal mice. Trafficking of Mst1$^{-/-}$ T cells to the peripheral LNs and spleen was reduced to one fourth and one third, respectively, of control T cells (Figure 2A). Mst1$^{-/-}$ B-cell trafficking to the LN was also reduced to one fourth compared with that of control B cells (Figure 2A). These data suggest that hypoplastic lymphoid tissues are due to impaired homing capacity of Mst1-deficient lymphocytes.

We examined attachment to the HEV for control and Mst1$^{-/-}$ lymphocytes simultaneously by intravital microscopy. Although accumulation of attached control T cells (green) on the HEV in the mesenteric LN was obvious 20 min after transfer, Mst1$^{-/-}$ T cells (red) poorly attached to the HEV (Figure 2B). We quantified the number of attached cells using images of several microscopic fields taken 30 min after cell transfer. The number of attached Mst1$^{-/-}$ T cells was decreased by approximately 65% compared with control cells (Figure 2B). Although B cells tended to be less efficient than T cells in attaching to the HEV, attachment of Mst1$^{-/-}$ B cells to the HEV was reduced by approximately 75% compared with control B cells (Figure 2B).

Impaired integrin-dependent firm adhesion of Mst1$^{-/-}$ T and B cells

Naive lymphocyte interaction to the HEV in peripheral LN is regulated by adhesive cascades initiated by L-selectin-

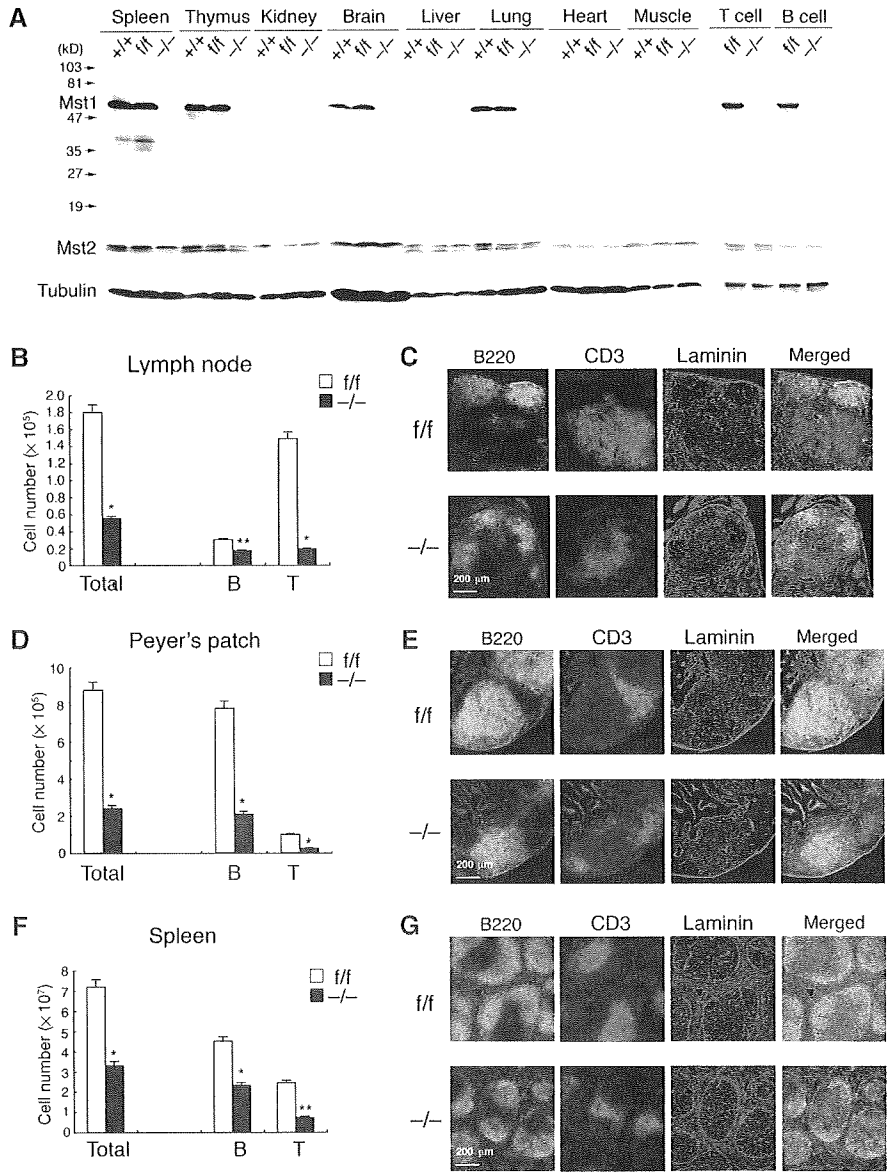

Figure 1 Hypoplastic lymphoid organs in Mst1-deficient mice. (**A**) Expression of Mst1 and Mst2 in organs of wild-type (+/+), $Mst1^{flox/flox}$ (f/f) and Cre^{+} $Mst1^{flox/flox}$ (−/−) mice. Tubulin served as a loading control. (**B**) Total and $CD3^{+}$ and $B220^{+}$ subset cell numbers in the inguinal lymph nodes. Total and subset numbers of axillary, popliteal, cervical and mesenteric lymph nodes in Mst1-deficient (−/−) mice were decreased to similar extents. $n=5$ for each, $^{*}P<0.001$, $^{**}P<0.005$, compared with the corresponding $Mst1^{flox/flox}$ (f/f) fractions. (**C**) Immunofluorescence staining of frozen tissue sections of axillary lymph nodes for B cells (B220; green), T cells (CD3; red) and laminin (blue). (**D**) Total and $CD3^{+}$ and $B220^{+}$ subset cell numbers in Peyer's patches. $n=5$ for each, $^{*}P<0.001$, compared with the corresponding $Mst1^{flox/flox}$ (f/f) fractions. (**E**) Immunofluorescence staining of frozen tissue sections of Peyer's patches for B cells (B220; green), T cells (CD3; red) and laminin (blue). (**F**) Total and $CD3^{+}$ and $B220^{+}$ subset cell numbers in spleens. $n=5$ for each, $^{*}P<0.01$, $^{**}P<0.005$, compared with the corresponding $Mst1^{flox/flox}$ (f/f) fractions. (**G**) Immunofluorescence staining of frozen tissue sections of the spleen for B cells (B220; green), T cells (CD3; red) and laminin (blue).

mediated tethering and rolling, followed by chemokine-triggered integrin activation and integrin-dependent arrest. Expression of L-selectin, LFA-1, α4 integrin and chemokine receptors CCR7 and CXCR4 was not affected in $Mst1^{-/-}$ lymphocytes (Supplementary Figure 4). To clarify specifically which step in the interaction with the HEV is impaired in $Mst1^{-/-}$ lymphocytes, we established an *in vitro* assay that reconstitute the lymphocyte adhesion cascade using endothelial cells (Kimura *et al*, 1999; Shamri *et al*, 2005) that express peripheral node addressin (PNAd) and ICAM-1, as intravital microscopic experiment was not found to be suitable for dissection of each step of adhesion cascades quantitatively. T cells were perfused into a parallel plate flow chamber coated with the endothelial monolayer with immobilized CCL21. The interactive processes were video-recorded and digitized with 30-ms intervals for a frame-by-frame cell tracking analysis. Representative profiles of the interactive processes were shown in Figure 3A. A fraction of T cell transiently attached, rolled and stopped under physiological shear stress (2–6 dyne/cm^2), whereas low shear stress (<0.5 dyne/cm^2) did not support rolling efficiently (data not shown), as reported before (Finger *et al*, 1996). As transition from the rolling to the arrest was best observed at 2 dyne/cm^2 in this system, the experiments were per-

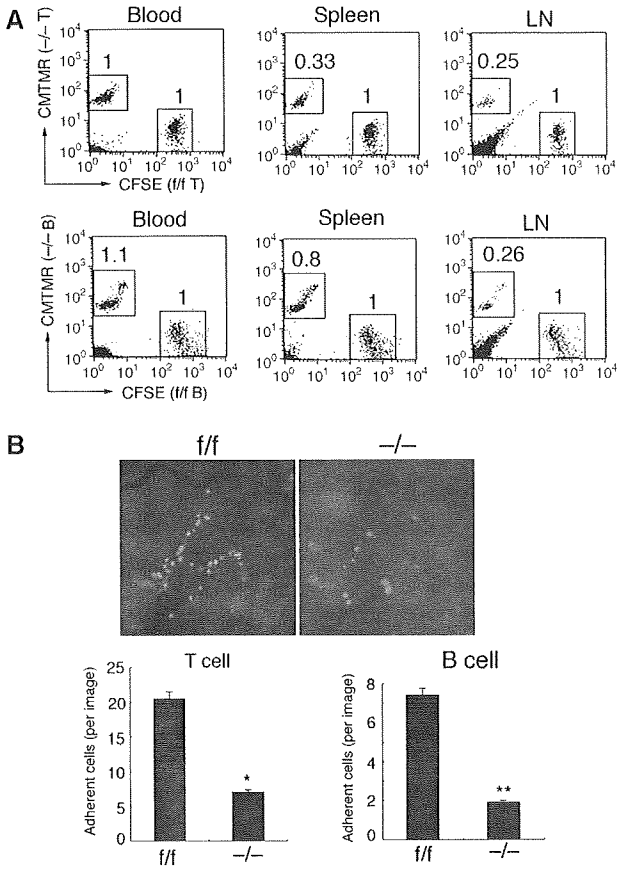

Figure 2 Defective homing of Mst1-deficient lymphocytes. (**A**) Adoptive transfer of T cells. T cells from $Mst1^{flox/flox}$ (f/f) and Mst1-deficient (−/−) mice were labelled with CFSE and CMTMR, respectively. They were mixed in equal numbers and injected into the tail veins of wild-type (Wt) mice. After 1 h, lymphocytes from the peripheral lymph nodes, spleen and blood were analysed by flow cytometry. Representative flow cytometry profiles of blood, lymph nodes, and spleen are shown. Numbers beside the boxed areas indicate the ratio of Mst1-deficient cells to $Mst1^{flox/flox}$ (f/f) cells (upper panel). Adoptive transfer of B cells. B cells from $Mst1^{flox/flox}$ (f/f) and Mst1-deficient (−/−) mice were similarly analysed as the T cells (lower panel). (**B**) Appearance of lymphocyte attachment to the HEV of the mesenteric lymph node. Intravital images of lymphocyte attachment to the HEV were taken 20 min after intravenous transfer of lymphocytes from $Mst1^{flox/flox}$ (f/f) (green) and Mst1-deficient (−/−) (red) mice (top). Representative images of three independent experiments are shown. The number of attached $Mst1^{flox/flox}$ (f/f) or $Mst1^{-/-}$ (−/−) T and B cells to the HEV. The number of attached cells were counted using images of more than five microscopic fields taken 30 min after cell transfer (bottom). Representative data of three independent experiments are shown. $*P<0.01$, $**P<0.005$, compared with the corresponding $Mst1^{flox/flox}$ (f/f) fractions. A full-colour version of this figure is available at *The EMBO Journal* Online.

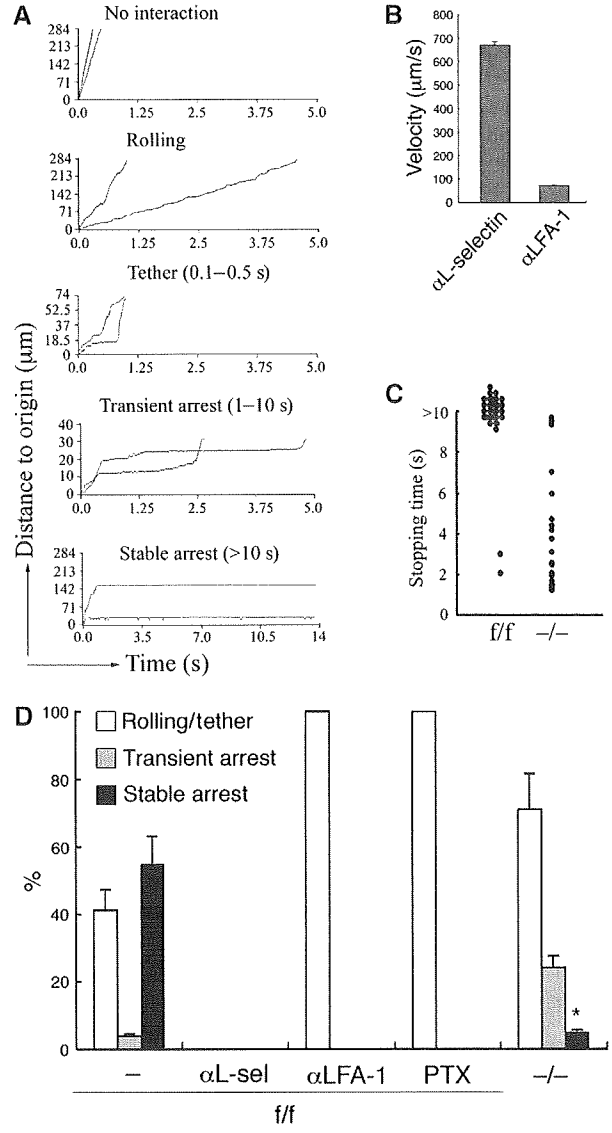

Figure 3 Defective integrin-dependent stable adhesion of Mst1-deficient lymphocytes. (**A**) Time-displacement profiles of individual T-cell movement over LS12 endothelial monolayers under shear flow. Primary T cells from control mice perfused at 2 dyne/cm^2 on LS12 monolayers immobilized with CCL21. Representative profiles of the cellular displacements over time were shown in four categories (no interaction, rolling, tether, transient and stable arrest), as described in the text. (**B**) The noninteracting and rolling velocities of control T cells movements on LS12 in the presence of anti-L-selectin and anti-LFA-1 antibody. (**C**) Stopping time of $Mst1^{flox/flox}$ (f/f) or Mst1-deficient (−/−) T cells arrested on LS12 endothelial cells were shown. More than 100 cells were measured in three independent experiments, and representative distribution of stopping time is shown. (**D**) Effects of anti-L-selectin, anti-LFA-1, PTX and Mst1-deficiency on the interactions of T cells with LS12 endothelial cells. Control $Mst1^{flox/flox}$ (f/f) T cells were pretreated with anti-L-selectin, LFA-1 and pertussis toxin (PTX), as described in Materials and methods. $Mst1^{flox/flox}$ (f/f) T cells and Mst1-deficient (−/−) T cells perfused at 2 dyne/cm^2 on LS12 monolayers, which was immobilized with CCL21. The adhesive events of >100 cells were measured and categorized as described in (A). Data represent the means and s.e.m. of three independent experiments. $*P<0.001$, compared with $Mst1^{flox/flox}$ (f/f) lymphocytes.

formed under this condition. The addition of anti-L-selectin antibody completely abolished adhesive events, as cells travelled at velocities approximately equivalent to theoretical velocities of noninteracting cells (>500 μm/s) (Figure 3A, B and D; Supplementary video 1). L-selectin-dependent interactions in the presence of anti-LFA-1 antibody resulted in a brief stop, which was <0.5 s (tether), or rolling with variable velocities (average 69.7 μm/s) (Figure 3A, B and D; Supplementary video 2). In the presence of immobilized CCL21, 60% of control T cells were attached to the endothelial cells for >1 s. A few cells detached within 10 s, but 94% of the attached cells stopped for >10 s, mostly over 2-min observation time (Figure 3C, D; Supplementary video 3). Therefore, we categorized the LFA-1-dependent adhesion into the transient (0.5–10 s) and stable arrest (>10 s), depending on dwell time on endothelial cells. As expected, PTX

treatment inhibited the arrest, both transient and stable, without affecting tether/rolling (Figure 3D), indicating that LFA-1 is activated by the intracellular signalling mediated through the Gi family. Mst1$^{-/-}$ T cells tethered and rolled normally, indicating that L-selectin-dependent adhesive interaction is not affected. However, the LFA-1-dependent adhesion was found to be unstable with >80% of Mst1$^{-/-}$ T cells were detached within 5 s (Figure 3C, D; Supplementary video 4), indicating that Mst1 plays a critical role in stabilization of the transient arrest.

We also examined under flow adhesion to the α4β7 ligand MAdCAM-1, the major ligand for homing to Peyer's patches. Control T and B cells displayed tethering/rolling, which efficiently resulted in stable arrest in the presence of chemokines (Supplementary Figure 5). Although the frequencies of the transient arrest were rather increased, both Mst1$^{-/-}$ T and B cells had defective stable arrest that was reduced to approximately one third of control cells (Supplementary Figure 5). Taken together, these data indicate that the reduced homing capacity of Mst1$^{-/-}$ lymphocytes is due to the impairment in stabilization of integrin-dependent arrest on HEV.

Mst1$^{-/-}$ lymphocytes are defective in LFA-1 clustering and talin accumulation at the contact sites

Under flow conditions, lymphocytes have to develop integrin-dependent stable adhesion within seconds. We also examined roles of Mst1 in the stabilization of lymphocyte adhesion under static conditions, in which cells might develop stable adhesion by other mechanisms. The lymphocytes were allowed to adhere to immobilized integrin ligands for several minutes before subjected to shear flow. Compared with control lymphocytes, there were few Mst1$^{-/-}$ T and B cells that exhibited shear resistant, firm attachment to ICAM-1 after a 10-min incubation in the presence of CCL21 for T cells and CXCR4 ligand CXCL12 for B cells (Figure 4A). The stable adhesion of both Mst1$^{-/-}$ T and B cells to the VLA-4 ligand VCAM-1 were also severely decreased (Figure 4B), compared with those of control T and B cells. Thus, Mst1 plays a nonredundant role in adhesion stabilization under static as well as flow conditions.

We reported earlier that Mst1 is required for cell polarization and LFA-1 clustering triggered by chemokines but not involved in the regulation of LFA-1 affinity changes measured by binding to soluble ICAM-1 (Katagiri *et al*, 2006). We examined whether an Mst1 deficiency in primary lymphocytes affected LFA-1 clustering and lymphocyte polarization in response to chemokines. T and B cells were treated with CCL21 and CXCL12 for 5 min in suspension and were then fixed and stained for LFA-1 and CD44. Approximately 20–25% of chemokine-stimulated T and B cells from control mice showed polarized morphologies with a leading edge and uropod, to which LFA-1 and CD44 were clustered, respectively (Figure 4C). Although talin tended to be accumulated at the leading edge, it was not precisely colocalized with clustered LFA-1 (data not shown). The majority of Mst1$^{-/-}$ T and B cells remained unpolarized, and the redistribution of LFA-1 was not clearly observed (Figure 4C). The defects in cell polarization and LFA-1 clustering were also observed when incubated on ICAM-1 in the presence of chemokines (Figure 4D). In control cells, LFA-1 clustering was observed at the contact sites on ICAM-1, where talin was colocalized (Figure 4D), in agreement with the important role of talin in the final common step of integrin activation (Tadokoro *et al*, 2003). In contrast, colocalization of LFA-1 with talin was not observed clearly on the contact site of Mst1$^{-/-}$ cells upon attachment to ICAM-1 (Figure 4D). These data suggest that the chemokine-triggered lymphocytes attach to ICAM-1 through LFA-1 clustering, and the impaired LFA-1 clustering in Mst1$^{-/-}$ cells result in defective talin recruitment to the contact sites, leading to unstable adhesion.

Reduced B-cell subsets and DC in the spleen

Segregation of T cells and follicular B cells in the peripheral LN requires chemokine signalling (von Andrian and Mempel, 2003), but the contribution of integrins to this process is unclear. In contrast, MZB cells were reported to localize in the marginal sinus of the spleen in a manner dependent on ICAM-1 and VCAM-1 (Lu and Cyster, 2002). MZB cells are characterized by high IgM and CD21 expression and low IgD and CD23 expression (Martin and Kearney, 2002). FACS analysis revealed that the B220^{+} CD21^{hi} CD23^{lo} population corresponding to MZB cells was scarcely present in Mst1$^{-/-}$ mice (Figure 5A). In control mice, IgM^{hi} IgD^{lo} MZB cells were clearly detected in the marginal sinus at the border between the white and red pulp of the spleen (Figure 5B). However, there were few cells at the corresponding sites in the spleens of Mst1$^{-/-}$ mice (Figure 5B). There were no irregular structures of the marginal sinus, which normally express ICAM-1, MAdCAM-1 and VCAM-1 (Supplementary Figure 6). These results support the notion that defective adhesion to ICAM-1 and VCAM-1 results in a MZB cell deficiency in Mst1$^{-/-}$ mice.

As Mst1 was expressed abundantly in BM-derived DCs (Supplementary Figure 7), we examined whether an Mst1 deficiency affected the adhesion of DCs. CD11^{+} splenic DCs were enriched from Mst1$^{-/-}$ and control mice and subjected to static adhesion assays using recombinant ICAM-1Fc or fibronectin. DCs from control mice adhered to ICAM-1 and fibronectin, but not substantially to BSA (Supplementary Figure 7). In contrast, Mst1$^{-/-}$ DCs poorly adhered to ICAM-1 and fibronectin. As LFA-1, VLA-4 and VLA-5 expression was comparable between control and Mst1$^{-/-}$ DCs (data not shown), these results indicate that splenic Mst1$^{-/-}$ DCs have defective stable adhesion. In the Mst1$^{-/-}$ spleen, the total number of CD11c^{+}B220^{-} conventional DCs (cDCs) was decreased to approximately 65% of the control spleen (Figure 5C). Among the three cDC subsets in the spleen, which are defined by the surface expression of CD4 and CD8 in addition to CD11c, CD8^{-}CD4^{+} and CD8^{-}CD4^{-}, DCs were substantially decreased (Figure 5C). CD11c^{+}B220^{+} plasmacytoid DCs were not affected in Mst1$^{-/-}$ mice (data not shown). CD11c^{+}CD8^{-} DCs are usually located at the bridging channel of the marginal zone and red pulp (Metlay *et al*, 1990), as was evident in the spleens of control mice (Figure 5D). In contrast, CD11c^{+} DCs were scarcely found in the bridging channel of the Mst1$^{-/-}$ spleen (Figure 5D). Marginal zone DCs are mobile with a high turnover rate (De Smedt *et al*, 1996); therefore, the deficiency of this DC subset could be due to impaired retention and/or homing caused by defective integrin function in Mst1$^{-/-}$ DCs.

Skin DC migration into draining LN was also found to be defective in Mst1$^{-/-}$ mice. In Mst1-deficient mice, the numbers of Langerhans DCs were equivalent to those of control

mice (Figure 5E). Skin DCs migrate into draining LNs at the peak 24 h after inflammatory stimulation such as painting of the skin with fluorescein isothiocyanate (FITC) (Macatonia *et al*, 1987; Katagiri *et al*, 2004). FITC$^+$ major histocompatibility complex (MHC) class II-positive DCs appeared in the draining LNs in control mice at 24 h after painting (Figure 5E). However, in Mst1-deficient mice, this population was reduced to 20% of that of control mice (Figure 5E), indicating that Mst1 is required for efficient trafficking of skin DCs to LNs.

Defective emigration of thymocytes

In the peripheral blood, the number of B cells was comparable between Mst1$^{-/-}$ mice and control mice, but T cells were reduced by approximately 60% (Figure 6A). On the other hand, thymic cellularity was significantly increased in Mst1$^{-/-}$ mice (Figure 6B). T-cell development was assessed by measuring surface expression of CD4 and CD8. Although CD4$^+$CD8$^+$ double-positive cells were modestly increased in number, single-positive CD4 and CD8 cells in Mst1$^{-/-}$ mice were increased in number and proportion by approximately two-fold, suggesting that T-cell maturation was not affected in Mst1$^{-/-}$ mice (Figure 6B and C). As impaired thymocyte egress could lead to an increase in mature, single-positive cells, we examined thymocyte egress in transwell assays using thymic lobes (Fukui *et al*, 2001). Both CD4 and CD8 single-positive cells from Mst1$^{-/-}$ mice displayed severe defects in emigration from the thymus in response to the

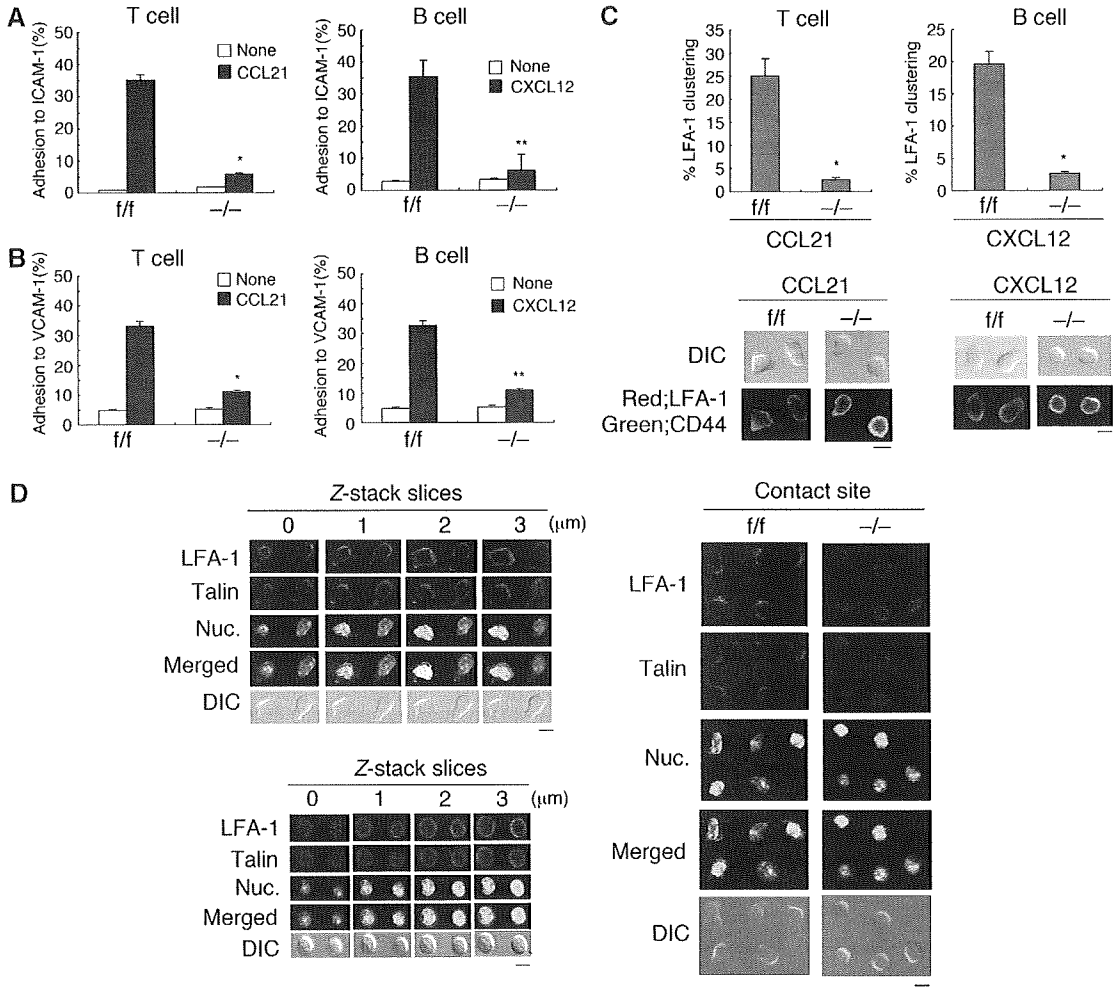

Figure 4 Defective stable adhesion and LFA-1 clustering in Mst1-deficient cells. (**A**) CCL21-stimulated T-cell adhesion (left) or CXCL12-stimulated B-cell adhesion (right) to ICAM-1. After incubation with 100 nM CCL21 or CXCL12 for 10 min, shear stress-resistant adhesion was measured as described in Materials and methods. Data represent the means and s.e.m. of triplicate experiments. None, no stimulation. $^*P<0.001$, compared with Mst1$^{flox/flox}$ (f/f) T cells stimulated with CCL21; $^{**}P<0.001$, compared with Mst1$^{flox/flox}$ (f/f) B cells stimulated with CXCL12. (**B**) CCL21-stimulated T-cell adhesion (left) or CXCL12-stimulated B-cell adhesion (right) to VCAM-1. Shear stress-resistant adhesion was measured as described above. Data represent the mean and s.e.m. of triplicate experiments. None, no stimulation. $^*P< 0.002$, compared with Mst1$^{flox/flox}$ (f/f) T cells stimulated with CCL21; $^{**}P<0.002$, compared with Mst1$^{flox/flox}$ (f/f) B cells stimulated with CXCL12. (**C**) Redistribution of LFA-1 (red) and CD44 (green). Mst1$^{flox/flox}$ (f/f) and Mst1-deficient (−/−) T and B cells were stimulated with CCL21 or CXCL12 for 5 min, then fixed and analysed by confocal microscopy quantitatively for cells showing a polarized distribution of LFA-1 and CD44 (top). Representative cell morphology and distribution of LFA-1 and CD44 (bottom). Data represent the means and s.e.m. of triplicate experiments. $^*P<0.001$, compared with Mst1$^{flox/flox}$ (f/f) lymphocytes. (**D**) Confocal microscopic analysis of LFA-1 and talin distribution of T cells from Mst1$^{flox/flox}$ (f/f) (left panel, upper) and Mst1-deficient (−/−) (left panel, bottom) mice. T cells were incubated on cover glass coated with ICAM-1 in the presence of CCL21 for 5 min, and then fixed and stained for LFA-1 and talin. DAPI was used for nuclear staining. A series of *Z*-stack images at 1-μm intervals from the glass surface are shown above (left panels). Right panels showed the LFA-1 and talin distribution on contact sites of Mst1$^{flox/flox}$ (f/f) and Mst1-deficient (−/−) T cells on ICAM-1.

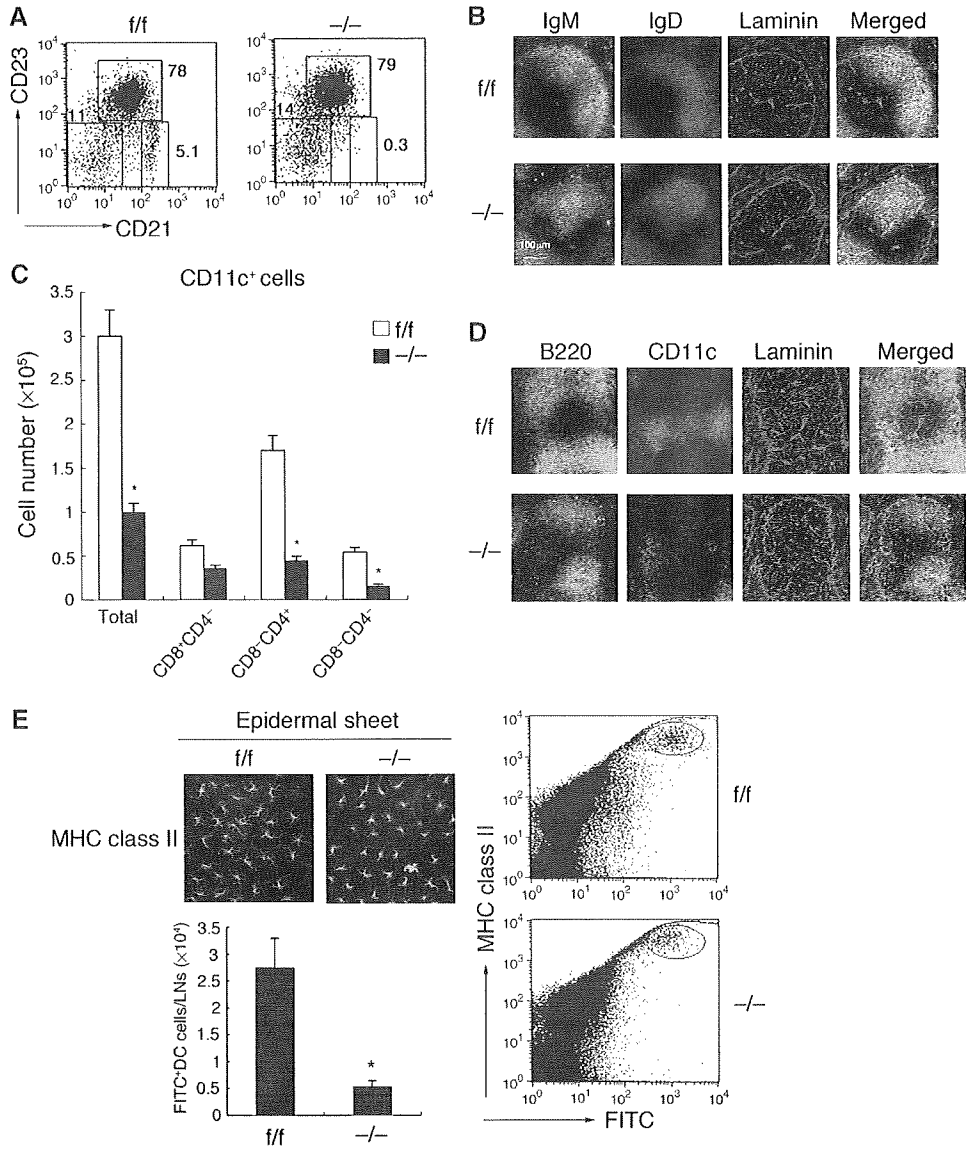

Figure 5 Deficient numbers of MZB cells and dendritic cells in the spleen of Mst1$^{-/-}$ mice. (**A**) Flow cytometry profiles of B220^{+} splenic B cells from Mst1$^{flox/flox}$ (f/f) and Mst1-deficient (−/−) mice stained with anti-CD21 and anti-CD23. The numbers beside the boxed areas indicate the percentages of CD21^{hi}CD23^{low} MZB cells, CD21^{hi}CD23^{hi} mature B cells and CD21^{-}CD23^{-} immature B cells of the total number of B220^{+} cells. (**B**) Spleen sections stained with IgM (green), IgD (red) and laminin (blue). IgM^{hi} and IgD^{-} marginal zone B cells were not observed in Mst1-deficient mice (bottom). (**C**) Total splenic DCs and numbers of splenic DCs in the CD8^{+}, CD8^{-}CD4^{-}, CD8^{-}CD4^{+} subsets. *$P<0.002$, compared with corresponding Mst1$^{flox/flox}$ (f/f) fractions. (**D**) Immunofluorescence staining of frozen tissue sections of Mst1$^{f/f}$ and Mst1$^{-/-}$ spleens for B cells (B220; green), DCs (CD11c; red) and laminin (blue). (**E**) Impaired DC trafficking from skin to draining lymph node. Epidermal sheets from Mst1$^{flox/flox}$ and Mst1-deficient mice stained with anti-MHC class II (upper, left panel). The number of skin-derived DCs migrated to lymph nodes after painting of shaved abdomens of Mst1$^{flox/flox}$ and Mst1-deficient mice with 1% FITC (lower, left panel). Data represent the absolute number of FITC^{+} MHC class II^{high} cells that appeared in draining lymph nodes (axillary and inguinal). $N=3$; *$P<0.005$. Representative flow cytometry profiles are presented in right panel.

CCR7 ligand CCL19 (Figure 6D). We also examined the apoptosis and proliferation of thymocytes. The proliferative response of Mst1$^{-/-}$ thymocytes to anti-CD3 was comparable to that of control thymocytes (data not shown). Although apoptosis of single-positive thymocytes was not affected, Mst1$^{-/-}$ double-positive thymocytes showed reduced apoptosis compared with control cells (45 ± 1.5 versus $34 \pm 1.5\%$, $P<0.02$), as judged by annexin V staining (Supplementary Figure 8). This reduction might contribute to a mild increase in double-positive thymocytes in Mst1$^{-/-}$ mice (Figure 6B). Thus, the accumulation of single-positive thymocytes is likely due to impaired thymic egress, which could lead to peripheral T-cell lymphopenia.

Defective lymphocyte interstitial migration

As combined defects in integrin clustering and cell polarization could lead to inefficient migration, we investigated whether the lack of Mst1 influenced lymphocyte interstitial migration. To this end, we first examined lymphocyte motility *in vitro*. As LN tissues are composed of an intricate network of stromal cells, which might support lymphocyte migration (Bajenoff *et al*, 2006), we used BLS12, a stromal cell line established from LNs (Katakai *et al*, 2004) (Katakai *et al*, 2008). As primary naive lymphocytes are generally immotile *in vitro*, we used cultured lymphoblasts in migration assays. T-cell blasts from control mice actively migrated on the BLS12

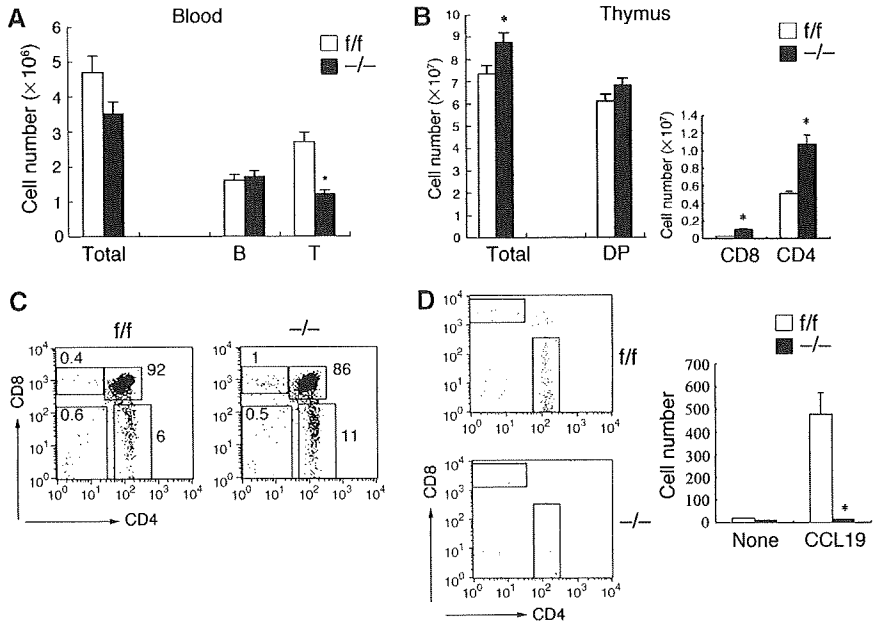

Figure 6 Decreased thymocyte emigration in Mst1-deficient mice. (**A**) Total and $CD3^+$ and $B220^+$ subset cell numbers in the peripheral blood of $Mst1^{flox/flox}$ (f/f) and Mst1-deficient (−/−) mice. $^*P<0.03$, compared with $Mst1^{flox/flox}$ (f/f) T lymphocytes. (**B**) Total, $CD4^+CD8^+$ double-positive (DP), $CD4^+$ or $CD8^+$ single-positive cells in thymi from $Mst1^{flox/flox}$ (f/f) and Mst1-deficient (−/−) mice. $^*P<0.05$, compared with the corresponding fractions. (**C**) CD4 and CD8 flow cytometry profiles of thymi from $Mst1^{flox/flox}$ (f/f) and Mst1-deficient (−/−) mice. The numbers beside the boxed areas indicate the percentages. (**D**) Emigration of thymocytes towards CCL19 from thymic lobes. Thymic lobes from $Mst1^{flox/flox}$ (f/f) or Mst1-deficient (−/−) mice were put in the upper chamber of transwell chemotactic chambers. CD4 and CD8 profiles of cells recovered from the lower chamber containing CCL19 were measured after 3 h (left), and the total numbers of emigrated cells (right) are shown. $^*P<0.001$, compared with $Mst1^{flox/flox}$ (f/f) single-positive cells.

monolayer with an average velocity of 8.1 ± 3.4 μm/min (Figure 7A; Supplementary video 5). This motility was reduced by approximately 39% after treating with anti-LFA-1 and anti-α4 integrin antibodies (data not shown). Compared with control cells, $Mst1^{-/-}$ T-cell blasts moved inefficiently with an average velocity of 5.2 ± 2.3 μm/min and a significantly reduced distance compared with control cells (Figure 7A; Supplementary video 6). Similarly, $Mst1^{-/-}$ B-cell blasts had impaired cell migration over the stromal layer with significant reductions in both velocity and displacement (Figure 7A; Supplementary videos 7 and 8). Control T- and B-cell blasts migrating over stromal layers displayed polarized phenotypes with a leading edge and uropod (Supplementary videos 5 and 7). However, most $Mst1^{-/-}$ T- and B-cell blasts failed to develop polarized cell shapes and displayed rather oscillated movements (Supplementary videos 6 and 8).

As chemokine-stimulated migration of lymphocytes includes integrin-independent processes (Lammermann *et al*, 2008), we also examined whether Mst1 could be involved in chemokine-dependent motility without integrin ligands (Woolf *et al*, 2007). Substantial numbers of control naïve T cells adhered and actively migrated on the immobilized CCL21 (Supplementary Figure 9). Mst1-deficient T cells attached similarly on the immobilized CCL21, but the motility was poor, compared with those of control cells (Supplementary Figure 9), suggesting that Mst1 is required for both integrin-dependent and -independent lymphocyte motility triggered by chemokines.

We then examined whether the Mst1 deficiency could influence primary naive lymphocyte motility within the LNs. A multiphoton microscopic analysis was performed using LN explants that had been adoptively transferred with differentially labelled lymphocytes from control and $Mst1^{-/-}$ mice (Figure 7B and C). As reported earlier (Miller *et al*, 2002; Stoll *et al*, 2002; Bousso and Robey, 2003; Mempel *et al*, 2004; Okada and Cyster, 2007), control T cells showed robust random walk-like movements within LN explants with an average velocity of 15.7 ± 4.2 μm/min (Figure 7B; Supplementary video 9). Under the same conditions, $Mst1^{-/-}$ T cells displayed inefficient migration; the average velocity was reduced by 40% (9.5 ± 4.8 μm/min), and the distance displaced from the initial tracking point was reduced by 68% compared with those of control T cells (Figure 7B; Supplementary video 9). B-cell migration was measured similarly by adoptive transfer of differentially labelled B cells from control and $Mst1^{-/-}$ mice. Most B cells were found in follicular areas. Compared with T cells, B cells were less motile with an average velocity of approximately 7.3 ± 2.6 μm/min (Figure 7C; Supplementary video 10), which was consistent with earlier reports (Miller *et al*, 2002; Han *et al*, 2005). $Mst1^{-/-}$ B cells had a reduced mean velocity of 4.5 ± 2.3 μm/min and decreased displacement (Figure 7C; Supplementary video 10). Taken together, these results indicate that Mst1 is required for efficient interstitial migration of both T and B cells.

Discussion

This study shows that the major role of Mst1 *in vivo* is to control lymphocyte adhesion and migration. T and B cells required Mst1 to attach firmly to the HEV when entering the LN. Mst1 deficiency in lymphocytes impaired their motility over stromal cells as well as within the intact LN. In addition

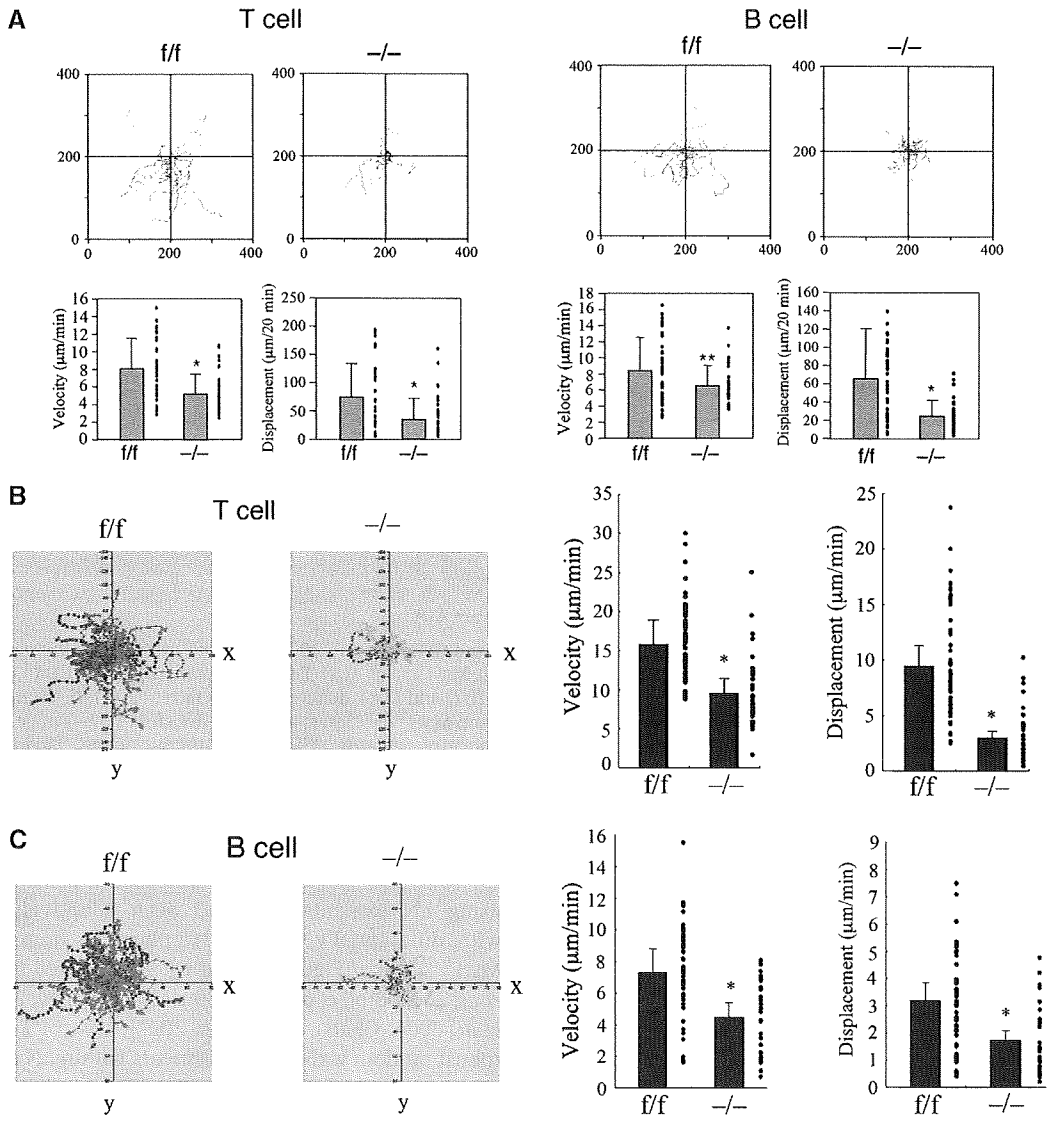

Figure 7 Defective interstitial migration of Mst1-deficient T and B cells. (**A**) Cell motility over monolayers of the BLS12 FRC cell line. Representative tracks of $Mst1^{flox/flox}$ (f/f) and $Mst1^{-/-}$ (−/−) T-cell blasts (left) and B-cells blast (right) over BLS12 cells as indicated (top). Each line represents a single cell track. Displacements and velocities of $Mst1^{flox/flox}$ (f/f) and Mst1-deficient (−/−) T and B cells (bottom). Sixty cells of each type were tracked for 10 min for each data set. The velocity data were obtained from movements every 30 s. $^{*}P<0.001$, $^{**}P<0.05$, compared with $Mst1^{flox/flox}$ (f/f) lymphocytes. (**B**) Multi-photon microscopic analysis of $Mst1^{flox/flox}$ (f/f) and Mst1-deficient (−/−) lymphocyte migration within LN explants. Representative tracks of $Mst1^{flox/flox}$ (f/f) T cells (red) and Mst1-deficient (−/−) T cells (green) are shown. Each line represents a single T-cell track (left). Velocities and displacements of $Mst1^{flox/flox}$ (f/f) and Mst1-deficient T cells (−/−) (right). Sixty-five cells of each type were tracked for each data set. $^{*}P<0.001$, compared with $Mst1^{flox/flox}$ (f/f) T cells. (**C**) Multi-photon microscopic analysis of $Mst1^{flox/flox}$ (f/f) and Mst1-deficient (−/−) B-cell migration as in (B). Representative tracks of $Mst1^{flox/flox}$ (f/f) B cells (red) and Mst1-deficient (−/−) B cells (green). Each line represents a single B-cell track (left). Velocities and displacements of $Mst1^{flox/flox}$ (f/f) and Mst1-deficient B cells (−/−) (right). Fifty-two cells of each type were tracked for each data set. $^{*}P<0.001$, compared with $Mst1^{flox/flox}$ (f/f) B cells. A full-colour version of this figure is available at *The EMBO Journal* Online.

to lymphocyte homing, Mst1 was required for localization of MZB cells and DCs in the marginal zone as well as thymocyte emigration. Thus, Mst1 is a key enzyme that controls proper immune cell localization and motility.

We previously identified Mst1 as a RAPL effector molecule that mediates integrin-dependent adhesion using lymphoid cell lines and lymphocytes (Katagiri *et al*, 2006). Our findings that the phenotype of Mst1-deficient mice was similar to that of RAPL-deficient mice (Katagiri *et al*, 2004) provides genetic evidence that indicates a critical link between Mst1 and RAPL in the regulation of lymphocyte trafficking. Although the phenotypes of these two mutant mice are similar, the phenotype of lymphocyte homing and lymphocytopenia in the peripheral LN appears to be more pronounced in $Mst1^{-/-}$ mice than $RAPL^{-/-}$ mice. As a RAPL deficiency reduced, but did not abrogate Mst1 phosphorylation (Katagiri *et al*, 2006), this may explain why the phenotype of Mst1-mutant mice is more severe than that of $RAPL^{-/-}$ mice.

Our study indicates that lymphocyte arrest is a transient process that must be sustained by intracellular signalling through Mst1. It is well established that the transition from leukocyte rolling to arrest is controlled by integrin activation through Gi signalling triggered by chemokines (Butcher *et al*, 1999). However, the development of a stable attachment from a nascent, labile attachment has not been recognized as an important process, which occurs within seconds as